20. Harikrishnan, K.N.; Chow, M.Z.; Baker, E.K.; Pal, S.; Bassal, S.; Brasacchio, D.; Wang, L.; Craig, J.M.; Jones, P.L.; Sif, S.; *et al.* Brahma links the SWI/SNF chromatin-remodeling complex with MeCP2-dependent transcriptional silencing. *Nat. Genet.* **2005**, *37*, 254–264.
21. Zhang, A.; Shen, C.H.; Ma, S.Y.; Ke, Y.; El Idrissi, A. Altered expression of Autism-associated genes in the brain of Fragile X mouse model. *Biochem. Biophys. Res. Commun.* **2009**, *379*, 920–923.
22. Chao, H.T.; Chen, H.; Samaco, R.C.; Xue, M.; Chahrour, M.; Yoo, J.; Neul, J.L.; Gong, S.; Lu, H.C.; Heintz, N.; *et al.* Dysfunction in GABA signalling mediates autism-like stereotypies and Rett syndrome phenotypes. *Nature* **2010**, *468*, 263–269.
23. Goncharova, E.A.; Goncharov, D.A.; Li, H.; Pimtong, W.; Lu, S.; Khavin, I.; Krymskay, V.P. mTORC2 is required for proliferation and survival of TSC2-null cells. *Mol. Cell. Biol.* **2011**, *31*, 2484–2498.
24. Nasuti, C.; Gabbianelli, R.; Falcioni, M.L.; di Stefano, A.; Sozio, P.; Cantalamessa, F. Dopaminergic system modulation, behavioral changes, and oxidative stress after neonatal administration of pyrethroids. *Toxicology* **2007**, *229*, 194–205.
25. Elwan, M.A.; Richardson, J.R.; Guillot, T.S.; Caudle, W.M.; Miller, G.W. Pyrethroid pesticide-induced alterations in dopamine transporter function. *Toxicol. Appl. Pharmacol.* **2006**, *211*, 188–197.
26. Kyoto Encyclopedia of Genes and Genomes. Available online: http://www.genome.jp/kegg/pathway/hsa/hsa05012.html (accessed on 9 January 2011).
27. Profiles of Chemical Effects on Cells system. Available online: http://project.nies.go.jp/eCA/cgi-bin/index.cgi (accessed on 28 February 2007).
28. Sone, H.; Okura, M.; Zaha, H.; Fujibuchi, W.; Taniguchi, T.; Akanuma, H.; Nagano, R.; Ohsako, S.; Yonemoto, J. Profiles of Chemical Effects on Cells (pCEC): A toxicogenomics database with a toxicoinformatics system for risk evaluation and toxicity prediction of environmental chemicals. *J. Toxicol. Sci.* **2010**, *35*, 115–123.
29. Gene Expression Omnibus. Available online: http://www.ncbi.nlm.nih.gov/projects/geo/query/acc.cgi?acc=GSE18503 (accessed on 10 October 2009).
30. Green, K.N.; Billings, L.M.; Roozendaal, B.; McGaugh, J.L.; LaFerla, F.M. Glucocorticoids increase amyloid-beta and tau pathology in a mouse model of Alzheimer's disease. *J. Neurosci.* **2006**, *26*, 9047–9056.
31. Arguelles, S.; Herrera, A.J.; Carreno-Muller, E.; de Pablos, R.M.; Villaran, R.F.; Espinosa-Oliva, A.M.; Machado, A.; Cano, J. Degeneration of dopaminergic neurons induced by thrombin injection in the substantia nigra of the rat is enhanced by dexamethasone: Role of monoamine oxidase enzyme. *Neurotoxicology* **2010**, *31*, 55–66.
32. Cummings, J.L.; Vinters, H.V.; Cole, G.M.; Khachaturian, Z.S. Alzheimer's disease: Etiologies, pathophysiology, cognitive reserve, and treatment opportunities. *Neurology* **1998**, *51*, S2–S17; discussion S65–S67.

33. van den Eeden, S.K.; Tanner, C.M.; Bernstein, A.L.; Fross, R.D.; Leimpeter, A.; Bloch, D.A.; Nelson, L.M. Incidence of Parkinson's disease: Variation by age, gender, and race/ethnicity. *Am. J. Epidemiol.* **2003**, *157*, 1015–1022.
34. van Dartel, D.A.; Pennings, J.L.; de la Fonteyne, L.J.; van Herwijnen, M.H.; van Delft, J.H.; van Schooten, F.J.; Piersma, A.H. Monitoring developmental toxicity in the embryonic stem cell test using differential gene expression of differentiation-related genes. *Toxicol. Sci.* **2010**, *116*, 130–139.
35. Chandler, K.J.; Barrier, M.; Jeffay, S.; Nichols, H.P.; Kleinstreuer, N.C.; Singh, A.V.; Reif, D.M.; Sipes, N.S.; Judson, R.S.; Dix, D.J.; *et al.* Evaluation of 309 environmental chemicals using a mouse embryonic stem cell adherent cell differentiation and cytotoxicity assay. *PLoS One* **2011**, *6*, doi:10.1371/journal.pone.0018540.
36. Gohlke, J.M.; Armant, O.; Parham, F.M.; Smith, M.V.; Zimmer, C.; Castro, D.S.; Nguyen, L.; Parker, J.S.; Gradwohl, G.; Portier, C.J.; *et al.* Characterization of the proneural gene regulatory network during mouse telencephalon development. *BMC Biol.* **2008**, *6*, doi:10.1186/1741-7007-6-15.
37. Zhao, L.; Morgan, M.A.; Parsels, L.A.; Maybaum, J.; Lawrence, T.S.; Normolle, D. Bayesian hierarchical changepoint methods in modeling the tumor growth profiles in xenograft experiments. *Clin. Cancer Res.* **2011**, *17*, 1057–1064.
38. Landers, J.P.; Bunce, N.J. The Ah receptor and the mechanism of dioxin toxicity. *Biochem. J.* **1991**, *276*, 273–287.
39. Gould, A.; Missailidis, S. Targeting the hedgehog pathway: The development of cyclopamine and the development of anti-cancer drugs targeting the hedgehog pathway. *Mini. Rev. Med. Chem.* **2011**, *11*, 200–213.
40. Okada, Y.; Shimazaki, T.; Sobue, G.; Okano, H. Retinoic-acid-concentration-dependent acquisition of neural cell identity during *in vitro* differentiation of mouse embryonic stem cells. *Dev. Biol.* **2004**, *275*, 124–142.
41. Vargesson, N. Thalidomide-induced limb defects: Resolving a 50-year-old puzzle. *Bioessays* **2009**, *31*, 1327–1336.
42. Rodier, P.M.; Ingram, J.L.; Tisdale, B.; Nelson, S.; Romano, J. Embryological origin for autism: Developmental anomalies of the cranial nerve motor nuclei. *J. Comp. Neurol.* **1996**, *370*, 247–261.
43. Stromland, K.; Nordin, V.; Miller, M.; Akerstrom, B.; Gillberg, C. Autism in thalidomide embryopathy: A population study. *Dev. Med. Child Neurol.* **1994**, *36*, 351–356.
44. Narita, M.; Oyabu, A.; Imura, Y.; Kamada, N.; Yokoyama, T.; Tano, K.; Uchida, A.; Narita, N. Nonexploratory movement and behavioral alterations in a thalidomide or valproic acid-induced autism model rat. *Neurosci. Res.* **2010**, *66*, 2–6.
45. Meerts, I.A.; Lilienthal, H.; Hoving, S.; van den Berg, J.H.; Weijers, B.M.; Bergman, A.; Koeman, J.H.; Brouwer, A. Developmental exposure to 4-hydroxy-2,3,3',4',5-pentachlorobiphenyl (4-OH-CB107): Long-term effects on brain development, behavior, and brain stem auditory evoked potentials in rats. *Toxicol. Sci.* **2004**, *82*, 207–218.

46. Stump, D.G.; Beck, M.J.; Radovsky, A.; Garman, R.H.; Freshwater, L.L.; Sheets, L.P.; Marty, M.S.; Waechter, J.M., Jr.; Dimond, S.S.; van Miller, J.P.; *et al.* Developmental neurotoxicity study of dietary bisphenol A in Sprague-Dawley rats. *Toxicol. Sci.* **2010**, *115*, 167–182.
47. Dalgaard, M.; Ostergaard, G.; Lam, H.R.; Hansen, E.V.; Ladefoged, O. Toxicity study of di(2-ethylhexyl) phthalate (DEHP) in combination with acetone in rats. *Pharmacol. Toxicol.* **2000**, *86*, 92–100.
48. Kakko, I.; Toimela, T.; Tahti, H. The synaptosomal membrane bound ATPase as a target for the neurotoxic effects of pyrethroids, permethrin and cypermethrin. *Chemosphere* **2003**, *51*, 475–480.
49. Numis, A.L.; Major, P.; Montenegro, M.A.; Muzykewicz, D.A.; Pulsifer, M.B.; Thiele, E.A. Identification of risk factors for autism spectrum disorders in tuberous sclerosis complex. *Neurology* **2011**, *76*, 981–987.
50. O'Roak, B.J.; State, M.W. Autism genetics: Strategies, challenges, and opportunities. *Autism Res.* **2008**, *1*, 4–17.
51. Muhle, R.; Trentacoste, S.V.; Rapin, I. The genetics of autism. *Pediatrics* **2004**, *113*, e472–e486.
52. Wang, J.; Rao, S.; Chu, J.; Shen, X.; Levasseur, D.N.; Theunissen, T.W.; Orkin, S.H. A protein interaction network for pluripotency of embryonic stem cells. *Nature* **2006**, *444*, 364–368.
53. Muller, F.J.; Laurent, L.C.; Kostka, D.; Ulitsky, I.; Williams, R.; Lu, C.; Park, I.H.; Rao, M.S.; Shamir, R.; Schwartz, P.H.; *et al.* Regulatory networks define phenotypic classes of human stem cell lines. *Nature* **2008**, *455*, 401–405.
54. *GeneSpring*, version GX10.02; Agilent Technologies: Palo Alto, CA, USA, 2010.

Cancer Biology & Therapy 13:5, 296-306; March 2012; © 2012 Landes Bioscience

Effects of bisphenol A exposure on the proliferation and senescence of normal human mammary epithelial cells

Xian-Yang Qin,[1,2,†] Tomokazu Fukuda,[3,†] Linqing Yang,[1,4] Hiroko Zaha,[1] Hiromi Akanuma,[1] Qin Zeng,[1] Jun Yoshinaga[2] and Hideko Sone[1,*]

[1]Health Risk Research Section; National Institute for Environmental Studies; Tsukuba, Japan; [2]Department of Environmental Studies; Graduate School of Frontier Science; University of Tokyo; Kashiwa, Japan; [3]Laboratory of Animal Breeding and Genetics; Graduate School of Agricultural Science; Tohoku University; Sendai, Japan; [4]Shenzhen Center for Disease Control and Prevention; Guangdong, China

[†]These authors contributed equally to this work.

Keywords: bisphenol A, cell growth, breast cancer, HMEC, methylation, cyclin E, p16

The carcinogenic activity of bisphenol A (BPA) is responsible for stimulating growth in estrogen-dependent breast cancer tissues, cell lines and rodent studies. However, it is not fully understood how this compound promotes mammary carcinogenesis. In our study, we examined the effect of BPA on cellular proliferation and senescence in human mammary epithelial cells (HMEC). Exposure to BPA for 1 week at the early stage at passage 8 increased the proliferation and sphere size of HMEC at the later stage up to passage 16, suggesting that BPA has the capability to modulate cell growth in breast epithelial cells. Interestingly, the number of human heterochromatin protein-1γ positive cells, which is a marker of senescence, was also increased among BPA-treated cells. Consistent with these findings, the protein levels of both p16 and cyclin E, which are known to induce cellular senescence and promote proliferation, respectively, were increased in BPA-exposed HMEC. Furthermore, DNA methylation levels of genes related to development of most or all tumor types, such as BRCA1, CCNA1, CDKN2A (p16), THBS1, TNFRSF10C and TNFRSF10D, were increased in BPA-exposed HMEC. Our findings in the HMEC model suggested that the genetic and epigenetic alterations by BPA might damage HMEC function and result in complex activities related to cell proliferation and senescence, playing a role in mammary carcinogenesis.

Introduction

Among the known estrogen-like compounds, bisphenol A (BPA) has received a great deal of attention, because it is commonly found in the environment, as well as in human tissues and fluids.[1,2] BPA has been detected in 92% of urine samples (0.4–149 μg/L) in a U.S. reference population, suggesting people may be continuously exposed to this compound in their daily lives.[3,4] Epidemiology studies have highlighted the correlation between BPA exposure and human cancers.[5] Animal studies have also shown that these low levels of BPA exposure may alter developmental programs of sensitive end organs during critical stages of early development, and increase mammary cancer risk in mouse models of breast cancer.[6,7]

The underlying mechanism involved in the carcinogenic activity of BPA has been studied in several animal and cell models. Betancourt et al.[8] demonstrated that changes in mammary gland protein expression of signaling pathways such as in the cell cycle, apoptosis, differentiation and migration are consistent with increased susceptibility for cancer development in rats prenatally exposed to BPA. Ptak et al.[9] also reported that exposure to environmental relevant concentrations of BPA can affect the cellular proliferation and expression of genes involved in the cell cycle and apoptosis in human ovarian cancer cells. However, studies with human breast cancer cells have yielded conflicting data,[10-12] and the molecular mechanisms by which exposure to BPA at the early passage can affect breast cells at later passages are still unknown.[13] Furthermore, to our knowledge, there are a lack of data concerning the action of BPA on gene expression involved in cell proliferation and apoptosis in normal human mammary endothelial cells (HMEC).

There is general consensus that accumulation of cellular damage is the initiating event of both cancer and aging.[14] Tumorigenesis is fuelled by the accumulation of genetic and epigenetic damage. Similarly, aging occurs, at least in part, because of an accumulation of macromolecular damage, which initially affects cellular proteins, lipids and DNA, but eventually impairs tissue regeneration. Accordingly, those mechanisms that protect cells from damage could, in principle, protect against cancer and aging simultaneously.[15] In this regard, one potential mechanism by which estrogenic agents such as BPA may promote carcinogenesis might include increased DNA damage.[16] DNA damage

*Correspondence to: Hideko Sone; Email: hsone@nies.go.jp
Submitted: 06/09/11; Revised: 12/02/11; Accepted: 12/02/11
http://dx.doi.org/10.4161/cbt.13.5.18942

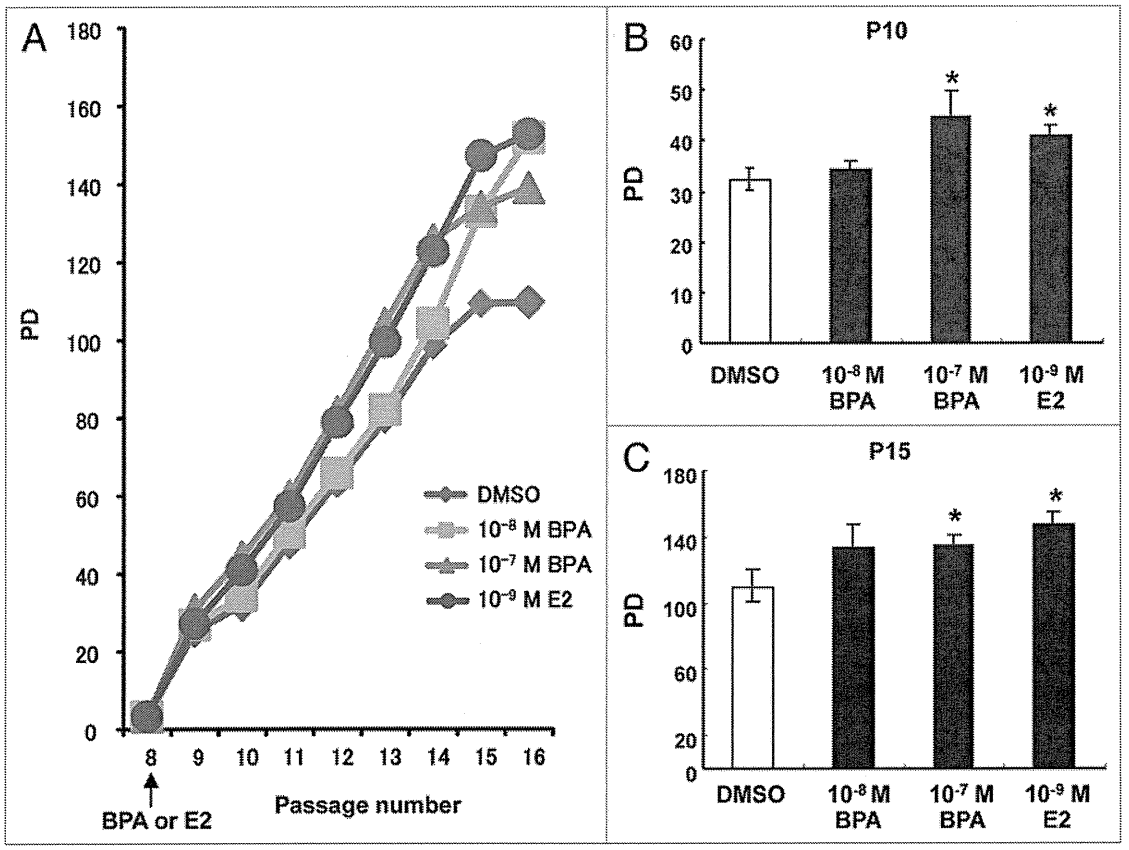

Figure 1. Effects of BPA exposure on the proliferation of HMEC. (A) Cumulative PDs of cells treated with DMSO, 10^{-7} M or 10^{-8} M BPA, or 10^{-9} M E2 at passage 8 (7 d period). Representative results from one series of experiments are shown. (B) Calculation of the PDs of HMEC at passages 10 and 15. *$p < 0.05$ vs. the DMSO control.

induced by 17β-estradiol (E2) is more than 1,000 times greater than that of BPA.[16] However, when BPA is compared with E2, a difference in biological effects is observed. For example, Bouskine et al. reported that the human testicular seminoma cell-promoting effect of BPA is mediated through two signaling pathways of estrogen receptors and G-protein-coupled receptors (GPCRs). The GPCR pathway is not activated by stimulation of E2. Therefore, it is likely that the effects of BPA are based on estrogenic activities, but are not identical to those of E2. To further elucidate the biological effects of BPA on the mammary gland, gene expression profiling has also been performed using in vivo animal models.[18] The resulting data indicated that a high dose of BPA induces changes in genes related to differentiation, suggesting that this compound may have an adverse effect on developmental processes in the mammary gland.[18] However, although gene expression profiles are very informative in terms of detecting expression changes in target organs, it is difficult to precisely determine the corresponding molecular mechanisms in various differentiated cells such as ductal epithelial, stromal and acinar cells in the in vivo system. To avoid issues of complexity when using in vivo systems, gene expression profiling has been performed using cultured cells treated with several environmental carcinogens.[19] In a similar manner, gene expression profiling following BPA exposure was performed in an earlier study using MCF-7 human breast cancer cells.[20] However, since MCF-7 cells are immortalized, they already harbor chromosomal abnormalities that are frequently observed in human malignant lesions.

In the current study, we evaluated the potential carcinogenic activity of BPA in HMEC, which are derived from normal human mammary epithelium, and therefore contain a normal karyotype.[21-23] The long-term effects of BPA exposure at "low doses" were focused on in this study, with a low dose currently considered as $< 2.19 \times 10^{-7}$ M for in vitro cell or organ culture studies.[24,25] We examined the effect of BPA exposure at early passage on proliferation, senescence, gene expression and DNA methylation in HMEC at later passages.

Results

Effects of BPA exposure on the proliferation of HMEC. An important aspect of our experimental design was to expose HMEC to BPA for 7 d at passage 8 and then examine its effects at later passages. Exposure to BPA and E2 enhanced cell proliferation of HMEC and increasing effects were still evident until passage 16, even after removing BPA and E2 from the cell culture medium from passage 9 (**Fig. 1A**). We statistically evaluated the differences in the speed of cell proliferation at the time points of

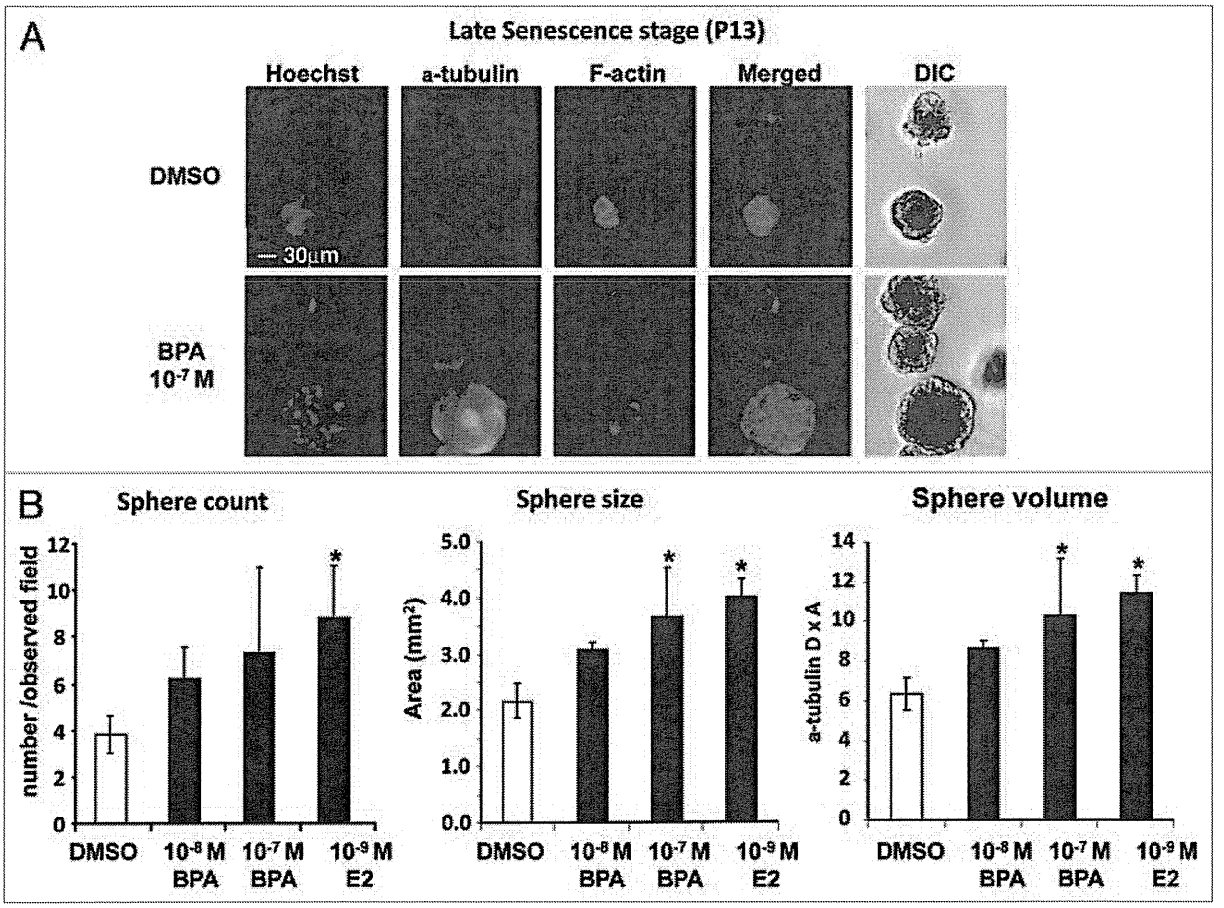

Figure 2. Effects of BPA exposure on colony formation of HMEC. Cells were treated with BPA or E2 at passage 8 (7 d period). (A) Morphology of colonies derived from HMEC at passage 13. Cells were stained with α-tubulin and F-actin antibodies. Cells were also counterstained with Hoechst, and the merged images and differential interference contrast (DIC) images are also shown (30 μm magnification). (B) Statistical analysis of sphere count, size and volume of colonies derived from HMEC at passage 13. *$p < 0.05$ vs. the DMSO control.

passages 10 and 15. As shown in **Figure 1B and C**, proliferation of HMEC was significantly enhanced through treatment with 10^{-7} M BPA and 10^{-9} M E2 at passage 10 and passage 15, respectively. These observations indicated that increased proliferation induced by exposure to BPA or E2 at an early passage persists during later cell divisions.

Effects of BPA exposure on the colony formation of HMEC. We found that BPA and E2 treatment enhanced cell proliferation, possibly also resulting in enhanced cellular senescence. To elucidate whether the enhanced cell proliferation by BPA and E2 had any effect on the carcinogenic status of HMEC, we employed a 3D "on-top" assay that offers the advantages of both 2D and 3D analysis.[27]

Cells covered with Matrigel produced rounded ductal colonies similar to spheres comprising a monolayer of epithelial cells, indicating that ductal formation had successfully occurred through coating with the Matrigel. The morphological status of HMEC at passage 13, which had been treated with BPA at passage 8, was assessed via the 3D "on-top" assay (**Fig. 2A**). Significant increases in sphere size of HMEC were found in the 10^{-7} M BPA and 10^{-9} M E2 treatment groups (**Fig. 2B**). The 3D "on-top" assay demonstrated that exposure to BPA and E2 at passage 8 can affect sphere formation in HMEC at later passages.

Recent studies have described that the balance between proliferation and senescence is important to develop cancer when normal cells are damaged by exogenous stimuli.[14,15] We then wished to determine whether BPA exposure could alter the balance between proliferation and senescence in HMEC. Therefore, we simultaneously examined the expression of cell cycle, proliferation and senescence markers in HMEC at passages 10 and 13, 2 to 5 weeks post-chemical treatment. Three-color fluorescence imaging analyses characterized the distribution of cells of various stages with Hoechst, HP1γ and BrdU (**Fig. 3A**). Hoechst staining indicates the number of nuclei in all cells. BrdU incorporation into nuclei represents identification of cells in the early S phase. HP1γ-positive cells at the early senescence stage (passage 10) were significantly increased by exposure to 10^{-7} M BPA (**Fig. 3B**, left part). At the late senescence stage (passage 13), a significant increase in HP1γ-positive cells was observed by exposure to both 10^{-8} M and 10^{-7} M BPA (**Fig. 3B**, right part). A significant increase in BrdU-positive cells was demonstrated by exposure to 10^{-8} M BPA at passages 10 and 13 (**Fig. 3C**).

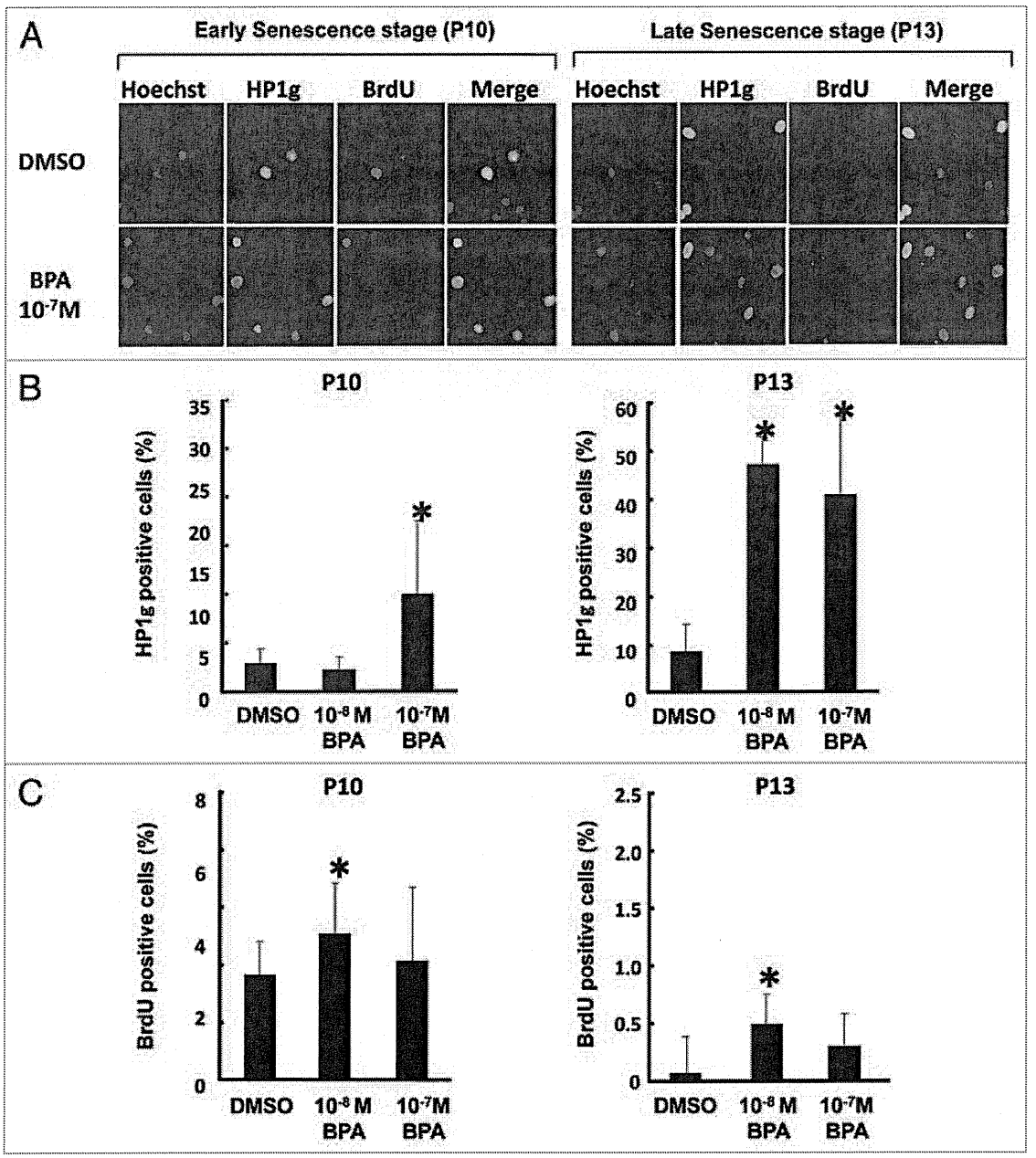

Figure 3. Effects of BPA exposure on cellular senescence of HMEC. Cells were treated with BPA at passage 8 (7 d period). (A) Staining of HMEC at passages 10 and 13 with HP1 γ or BrdU antibodies. Cells were also counterstained with Hoechst, and the merged images are also shown (200x magnification). (B) Number of HP1γ-positive cells. (C) Number of BrdU positive cells. *p < 0.05 vs. the DMSO control.

Gene and protein expression analysis. To determine the effects of BPA on the cellular growth of HMEC at the transcriptional level, gene expression analyses using a PCR array for mammary cancer-related genes were performed in HMEC at passage 11. Genes showing differential expression with BPA exposure are summarized in **Figure 4A**. It is noteworthy that the downregulated genes are associated with cell cycle control in many cases. A knowledge-based gene interaction network was then analyzed to determine how BPA at a dose of 10^{-8} M plays a role in signaling associated with cell cycle control (**Fig. 4B**). *CCNE1*, *CCNA2* and *CDKN2A*, which are among the key molecules underlying G_1-S control during the cell cycle, were downregulated or unchanged in BPA-treated HMEC. Other factors related to cell growth such as *EGFR*, *ERBB2*, *PTGS2* and *IGFBP2* were increased by BPA treatment at 10^{-8} M or 10^{-7} M (**Fig. 4A**). These observations indicate that the increased proliferation we observed in the BPA-treated cells may have been due to enhanced G_1-S progression resulting from the decreased expression of negative cell cycle regulators.

Knowledge-based network analysis was then performed to further clarify these findings. Network analysis for gene expression profiling at 10^{-8} M of BPA found that Tp53 upregulated CDKN2A and CCNA2, and indirectly interacted with CCNE1, and that the

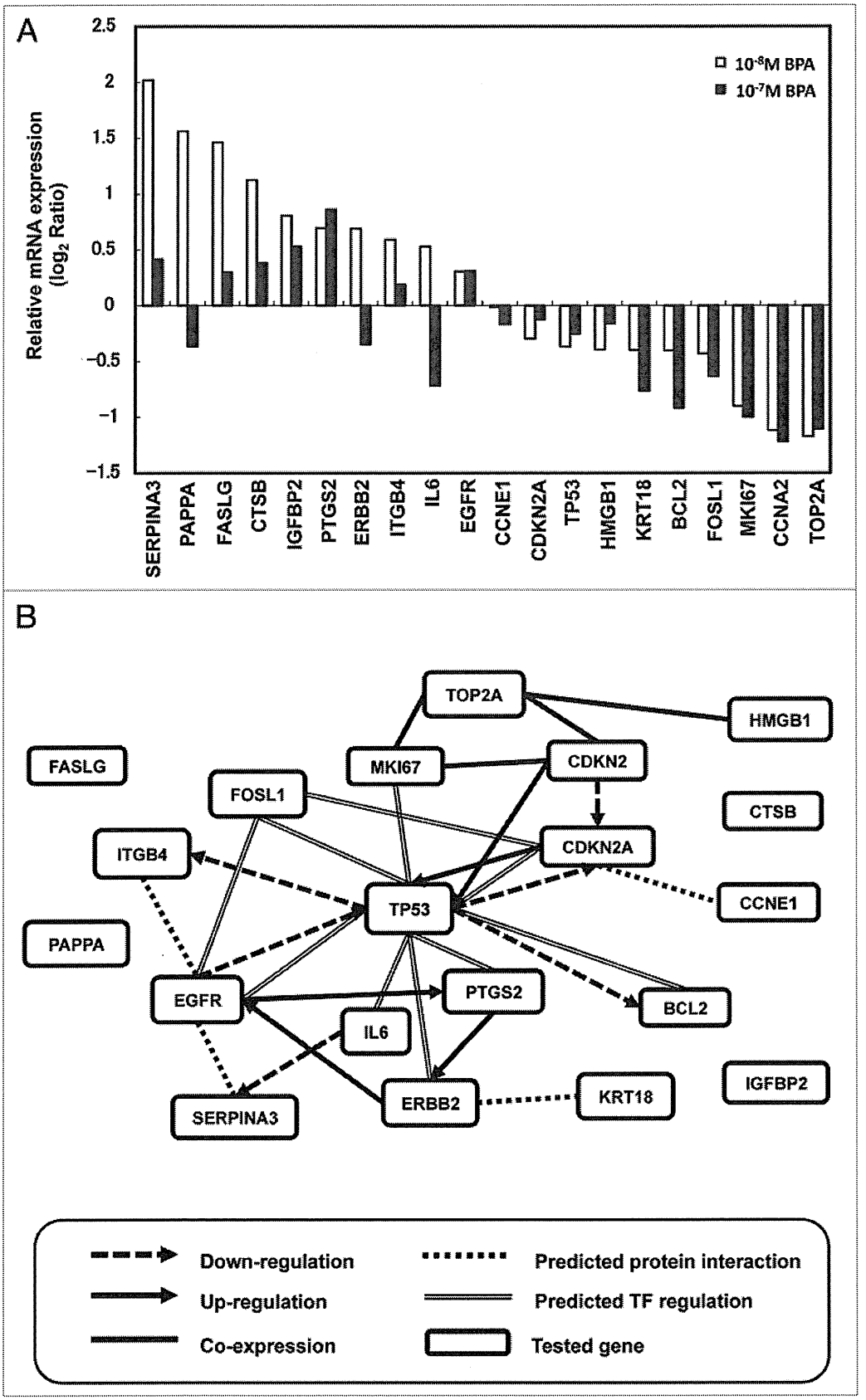

Figure 4. For figure legend, see page 301.

Figure 4 (See previous page). Gene expression and network analysis. HEMC were treated with BPA or E2 at passage 8 (7 d period) and the relative mRNA expression of selected genes was measured at passage 11. (A) Effects of BPA exposure on cancer signaling gene expression. The results are expressed as the average of two independent experiments. Relative mRNA expression normalized to β-actin is shown as the log2 ratio, with the fold-change referring to the DMSO control cells. (B) Gene networks representing key genes for BPA exposure at 10^{-8} M were identified using GNCPro (SA Biosciences).

upregulation of FASLG, CTSB, IGFBP2 and PAPPA were not associated with TP53.

We also investigated the effects of BPA exposure on protein expression of p16 (CDKN2A), p53 (TP53) and Cyclin E (CCNE1) in HMEC using western blot analysis. As shown in **Figure 5**, BPA exposure did not have a significant effect on p53 protein expression, while a dose-dependent increase in p16 protein expression was observed. Downregulation at 10^{-8} M BPA and upregulation at 10^{-7} M BPA of Cyclin E protein expression were also observed.

DNA methylation patterns. Alterations in DNA methylation patterns are associated with the development of a variety of human cancers, including breast cancer.[28,29] Previous studies have found promoter hypermethylation of in situ lesions and identified aberrant methylation at the promoters of candidate genes, which include *GSTP1, CCND2, RARB2, TWIST1, RASSF1A, HIC1, CDKN2A, SFN (TP53), BRCA1, CCNA1, THBS1, TNFRSF* and *APC1*.[30-33] Therefore, BPA-induced changes in the methylation status of 24 gene promoters were investigated via quantitative real-time PCR arrays in this study. **Table 1** shows that seven gene promoters exhibited changes of more than 10% in hypermethylation status between DMSO control and BPA-exposed cells (**Table 1**). These genes exhibited an increased percentage of promoter hypermethylation by BPA exposure including *BRCA1, CCNA1, CDKN2A, THBS1, TNFRSF10C* and *TNFRSF10D*, while *HIC1* had decreased promoter hypermethylation by BPA exposure.

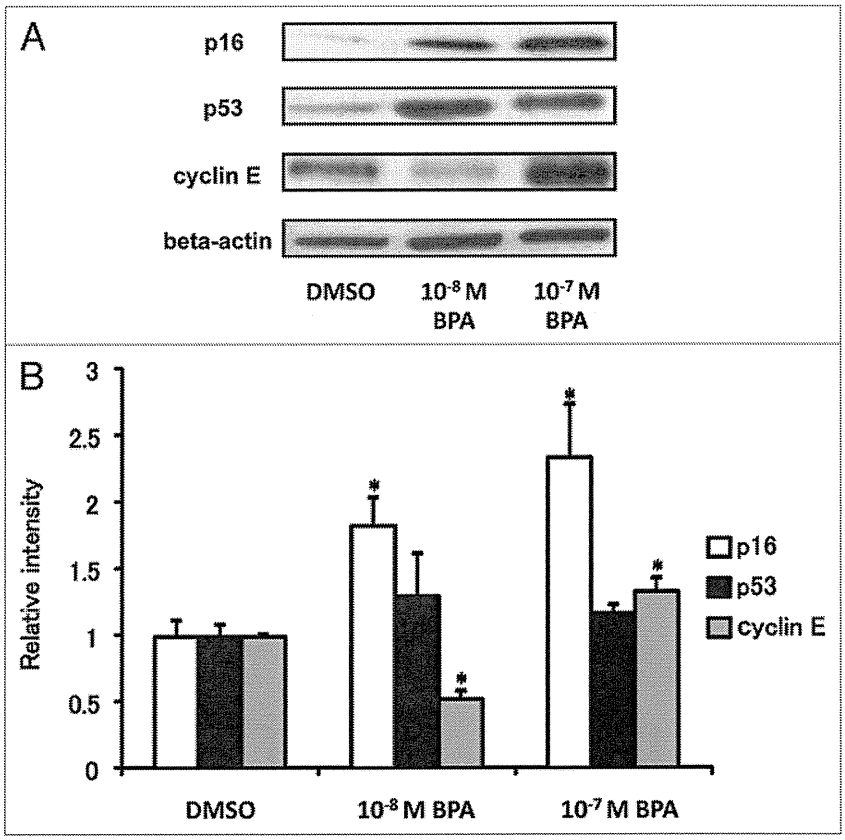

Figure 5. Modulation of the protein expression of p16, p53 and cyclin E in HEMC by BPA exposure. (A) Cells were treated with 10^{-8} M or 10^{-7} M BPA at passage 8 (7 d period) and protein expression of p16, p53 and cyclin E was measured at passage 11. (B) The cellular protein levels were calculated using ImageJ densitometry software and are expressed as the mean ± SD relative to DMSO control after normalizing the bands to β-actin. *$p < 0.05$ vs. the DMSO control.

Discussion

To investigate how BPA affects the carcinogenesis process in normal breast cells, we exposed HMEC to this agent at an early passage for a duration of 1 week and examined subsequent effects on cell proliferation, gene expression and DNA methylation at the stage of later passages. HMEC are a model system for studying early events in mammary tumorigenesis, and they have a normal karyotype and enter senescence after a lengthy culture, while neoplastic cells are allowed to continuously grow, thus overcoming the barrier of cellular senescence.[34] HMEC morphology and growth status in in vitro culture assay have been shown to be closely connected with malignancy in a comparison involving 25 mammary-gland-derived cell lines.[27]

In the current study, we focused on the effects of early-passage exposure to BPA in later-passage HMEC. In non-treated HMEC, the rate of cell growth slowed at approximately passage 15 (**Fig. 1A**), indicating the onset of cellular senescence, as HMEC are not immortalized. In contrast, HMEC treated with E2 or BPA did not show a reduced cell proliferation rate at approximately passage 15 (**Fig. 1A**). Our previous study showed that the telomerase activity of BeWo cells was enhanced by their exposure to E2 or 2,3,7,8-tetrachlorodibenzo-*p*-dioxin, a known endocrine disrupting agent.[35] This suggests that BPA might also upregulate telomerase activity in HMEC, resulting in an extended lifespan until a crisis point is eventually reached and cell division ceases.

To clarify the effects of BPA and E2 treatment on cell growth, a 3D "on-top" assay was performed using Matrigel, which is the optimal coating material for HMEC in this assay. Our optimized 3D "on-top" assay showed that BPA and E2 enhanced the

Table 1. Promotor methylation status of genes in HMEC at passage 12

Symbol	Ref Seq	DMSO			BPA 10^{-8} M			Differences (BPA-DMSO)		
		HM	UM	IM	HM	UM	IM	HM	UM	IM
BRCA1	NM_007294	3.4%	96.6%	0.0%	24.5%	75.5%	0.0%	21.2%	-21.2%	0.0%
CCNA1	NM_003914	7.2%	92.8%	0.0%	36.0%	64.0%	0.0%	28.8%	-28.8%	0.0%
CCND2	NM_001759	11.5%	29.2%	59.3%	12.8%	47.3%	40.0%	1.3%	18.0%	-19.3%
CDKN2A#	NM_058195	3.8%	96.2%	0.0%	16.7%	83.3%	0.0%	12.9%	-12.9%	0.0%
CDKN2A#	NM_000077	5.0%	8.3%	86.7%	19.3%	28.3%	52.4%	14.3%	20.0%	-34.3%
GSTP1	NM_000852	3.0%	97.0%	0.0%	2.3%	55.9%	41.9%	-0.8%	-41.1%	41.9%
HIC1	NM_006497	97.2%	2.8%	0.0%	68.2%	31.8%	0.0%	-29.0%	29.0%	0.0%
THBS1	NM_003246	5.5%	94.5%	0.0%	36.9%	63.1%	0.0%	31.4%	-31.4%	0.0%
TNFRSF10C	NM_003841	12.5%	54.9%	32.6%	24.8%	75.2%	0.0%	12.2%	20.4%	-32.6%
TNFRSF10D	NM_003840	5.1%	94.9%	0.0%	17.7%	82.3%	0.0%	12.6%	-12.6%	0.0%

HM, hypermethylated; UM, un-methylated, IM intermediately methylation. Cells were treated with vehicle (DMSO) and 10^{-8} M BPA at passage 8 (7 d period). #indicated that different probes of the promoter region of *CDKN2A* were used in this assay.

nuclear count for each HMEC colony and increased the area of these colonies at passage 13. Kenny et al.[27] reported morphological differences among colonies under 3D "on-top" analysis of 25 mammary cancer-derived cell lines, and they could be classified into four groups of "round," "mass," "grape-like" and "satellite." Relatively fewer malignant cells show round-shaped colonies in the 3D "on-top" assay, and most malignant grades result in grape-like or satellite shapes.[27] In our study, HMEC showed a "mass" shape (**Fig. 2**), and treatment with BPA or E2 did not change the shape of the colonies, but increased the size and cell numbers for each colony. These results indicated that BPA exposure at passage 8 had a subsequent effect on the cell growth of HMEC. The increased nuclear count and body area of spheres indicated overgrowth of the differentiated colony, possibly indicating a hyperplastic state. This may provide a key insight into the potential adverse effects of BPA upon the status of the mammary gland, which may result in carcinogenesis.

BPA exposure was found to increase the number of HP1γ-positive cells in HMEC at passages 10 and 13 in our study (**Fig. 3A and B**). At the late senescence stage (passage 13), both 10^{-8} M and 10^{-7} M BPA exposure increased HP1γ-positive cells but not BrdU-positive cells. A previous study reported that the onset of senescence induces an increase in the number of positive nuclear bodies that contain HP1γ.[36,37] HP1γ protein is also known to be positive for the entire nuclear area in the early S stage[38] and the G_2/S stage of the cell cycle.[39,40] When non-immortalized cells are close to their cell division limit, they often show positive SA-βgal activity in the cytoplasm and senescence-associated DNA foci in nuclei containing HP1γ.[37] Therefore, there are several possible explanations for the increased nuclear HP1γ-positive nuclei by BPA exposure in this study, such as enhanced cellular senescence or a delayed cell cycle progression during the G_1/S stage.

To elucidate the effects of BPA on enhanced cellular senescence or a delayed cell cycle progression during the G_1/S stage in HMEC, gene and protein expressions of mammary cancer-related genes were investigated in this study. Cyclin E protein expression was increased by exposure to BPA at the high dose (10^{-7} M), but not at the low dose (10^{-8} M) (**Fig. 5**). This might partly explain our findings that BPA exposure at the high dose but not the low dose at passage 8 significantly increased HEMC growth at passages 10 and 13 (**Fig. 1B and C**). Cyclin E is cyclically expressed during the cell cycle, and it binds and activates the cyclin-dependent kinase Cdk2 and catalyzes the transition from the G_1 phase to the S phase.[41,42] Our findings suggest that Cyclin E might play an important role in BPA-induced cell growth of HMEC. However, a discrepancy between Cyclin E gene and protein expression following BPA treatment was observed in our study (**Figs. 4A and 5**). The regulation of Cyclin E is through transcriptional regulatory mechanisms or through protein degradation by the proteasome pathway.[43] It is known that SCF (Skp1-Cullin-F-box) ubiquitin ligases regulate the degradation of many proteins involved in the control of cell division and growth.[44,45] Indeed, it has been reported that the amount of Cyclin E protein present in the cell is tightly controlled by ubiquitin-mediated proteolysis and one ubiquitin ligase responsible for Cyclin E ubiquitination is known as SCF^{Fbw7}.[46,47] Furthermore, it was found that phosphorylation within N- and C-terminal legions of Cyclin E plays a critical role in the binding of Cyclin E to SCF^{Fbw7} and thus its ubiquitination and proteasomal degradation.[48] Therefore, one possible explanation of our results is that BPA exposure might affect the phosphorylation of Cyclin E. Interestingly, a recent study that analyzed the effects of a low dose of BPA in a testicular cell line revealed that this compound induces the activation of cAMP response-element-binding protein and strongly induces the phosphorylation of retinoblastoma protein (Rb).[17] These findings support our hypothesis that the effect of BPA exposure on mammary cell proliferation is related with the dysregulation of cell cycle regulatory genes, since the activation of Rb is also known to enhance the cell cycle, particularly at the G_1-S transition. An animal study recently found that BPA exposure can significantly accelerate mammary tumorigenesis and metastasis in MMTV-erbB2 mice, and one of the underlying mechanisms includes the regulation of phosphorylation of proteins involved in the Akt pathway.[49] Because the overexpression of Cyclin E has been related to progression of a variety of cancers and constitutive expression of Cyclin E leads to genomic instability, further

study on the mechanism by which long-term BPA exposure could mediate Cyclin E expression might provide an insight into the potential carcinogenic activity of BPA in the mammary gland.

Another interesting finding of our study is that BPA exposure appeared to promote cellular senescence and proliferation of HEMC simultaneously (**Figs. 1–3**). This was supported by our findings that BPA exposure increased p16 protein expression in a dose-dependent manner; p16 has recently been found to promote aging in murine cells.[50] Indeed, there has been increased attention on the balance between convergent and divergent mechanisms of cancer and aging.[14,15] Both cancer and aging are fuelled by the accumulation of cellular damage. Additionally, one concern regarding BPA is that differing doses of BPA may function in distinctly different, and sometimes opposing, manners at both the tissue and molecular level.[49] Our study suggests that effects of BPA exposure at differing doses on the balance of cancer and aging in the mammary gland might partly contribute to this issue.

Eckhardt et al.[51] reported that approximately one-third of the differentially methylated 50-UTRs were inversely correlated with transcription in normal tissues. Radpour et al. and other researchers also reported that 10 hypermethylated genes (*APC*, *BIN1*, *BMP6*, *BRCA1*, *CST6*, *ESRb*, *GSTP1*, *CDKN2A*, *CDKN1A* and *TIMP3*) were identified for distinguishing between cancerous and normal tissues.[52-54] Therefore, hypermethylation of tumor suppressor genes causes the inactivation of genes that are important in suppressing the development of most or all tumor types. In our study, we observed increases in DNA hypermethylation of *BRCA1*, *CCNA1*, *CDKN2A*, *THBS1* and *TNFRSF* in BPA-exposed HMEC (**Table 1**). We were interested in *CDKN2A* hypermethylation status by exposure to BPA because *CDKN2A* and *GSTP1* showed significantly ($p < 0.002$) higher mean methylation levels in increasing grades (I, II, III) of invasive ductal breast cancer in a study by Moelan et al. Interestingly, both of the two *CDKN2A* probes increased levels of DNA hypermethylation by exposure to BPA, although DNA hypermethylation levels of *GSTP1* were not altered in our study. *CDKN2A* (p16), an inhibitor of the cyclin D-dependent protein kinases, is a tumor suppressor gene, and is altered in several tumor types.[56] Correlation of *CDKN2A* hypermethylation with CDKN2A protein loss has been previously reported and its loss of function has been associated with the development of a variety of cancers.[56-58] Our finding is inconsistent with these previous studies, which found that exposure to BPA in HMEC at passage 8 induced CDKN2A protein expression at passage 11 and promoter hypermethylation at passage 12. However, a study using tumor tissues derived from patients diagnosed with endometrial carcinoma found that loss of nuclear p16 protein expression is not associated with promoter methylation.[59] Our study indicates that the mechanism by which BPA upregulates CDKN2A protein expression appears to be complicated and further study is required for clarification.

In summary, our present study is the first to address the long-lasting effects of BPA exposure over multiple cellular passages of HMEC. The underlying mechanism might include genetic and epigenetic dysregulation of cell cycle regulatory genes or tumor suppressor genes.

Materials and Methods

Chemicals. Dimethyl sulfoxide (DMSO) and E2 were obtained from Sigma Chemical Co. BPA was obtained from Wako Industries. DMSO was used as the primary solvent for all chemicals, and DMSO solutions were further diluted in cell culture media for treatment. The final concentrations of DMSO in the media did not exceed 0.1% (vol/vol).

Cell culture and chemical treatment. HMEC were obtained from Cambrex Bio Science and maintained in accordance with the supplier's instructions. Briefly, the cells were cultured in plastic dishes with MEGM SingleQuots medium in an incubator at 37°C in 5% CO_2. HMEC were supplied at passage 7, and were grown to passage 8 prior to use in the experiments. BPA at final concentrations of 10^{-7} M and 10^{-8} M or E2 at 10^{-9} M was added to the culture media of passage 8 in HMECs and maintained for a period of 1 week. During this week, the culture media were changed twice with media containing the original BPA concentrations. The culture was then further grown until it was harvested for phenotype and gene expression analysis in media without chemicals. The cumulative population doublings (PDs) as a determinant of cellular lifespan were measured as previously described in reference 26. Briefly, the total number of cells harvested from each subculture was calculated and the number of accumulated PDs per passage was determined by the equation PD = (A/B)/log2, where A is the number of harvested cells and B is the number of plated cells.[26] Data were obtained from 6 duplicate cultures at each passage. The cumulative PDs from passage 8 to 16 were measured twice to validate the reproducibility of the results. The 3D "on-top" in vitro culture assay was performed essentially as described previously with different biocoated plates[27] (BD BioCoat Cellware Matrigel or Collagen Type I Coated Cellware plate, BD Biosciences).

Immunofluorescence cytochemistry. HMEC were transferred to 3D culture systems at passage 11 and maintained until passage 13. HMEC were then fixed in 4% neutralized paraformaldehyde solution for 60 min and blocked with 3% normal goat serum (NGS)/0.5% Triton X-100 in phosphate-buffered saline (PBS). The primary antibodies used were mouse monoclonal antibodies for human heterochromatin protein-1γ (HP1γ, S-19; Santa Cruz Biotechnology, sc-101004), and a rabbit polyclonal antiserum to α-tubulin (Abcam, ab15246). The secondary antibodies were anti-mouse Alexa 546 and Alexa Fluor 488 goat anti-rabbit IgG antibodies (Invitrogen). For the measurement of 5-bromo-2'-deoxyuridine (BrdU) incorporation during DNA synthesis, a cell proliferation fluorescence kit (GE Healthcare, 25-9001-89) was used according to the instruction manual. DNA was visualized by Hoechst staining (Wako Industries) and F-actin was visualized using Alexa Fluor 568 phalloidin (Invitrogen). Immunofluorescence staining signals were detected with an IN Cell Analyzer 1000 (GE Healthcare), a multiple-imaging analyzer, and morphological analysis was performed using IN Cell Investigator image analysis software (GE Healthcare).

Gene expression analysis. Total RNA was extracted using an RNeasy kit (Qiagen) when cells at passage 11 were approximately

70% confluent. These preparations were then used to detect the expression of 83 genes (**Table S1**), which have been reported to be frequently expressed in mammary cancers using a real-time RT-PCR method, Superarray-qPCR (Estrogen Receptor Signaling PCR Array, SA Biosciences). Gene expression was normalized by β-actin expression and set to 1 for the control DMSO-treated cells.

Western blot analysis. HMEC treated with BPA for a period of 1 week at passage 8 were lysed at passage 11 using RIPA buffer (Santa Sruz Biotechnology). After boiling at 99°C for 5 min, the protein samples were resolved by sodium dodecyl sulfate (SDS) PAGE on a 4–20% gel and transferred to a polyvinylidene difluoride membrane (Bio-Rad Laboratories). After blotting in tris-buffered saline (TBS) with 5% nonfat dry milk-Tris buffered saline and 0.1% Tween, the membrane was probed with p16 (1:10,000 dilution, Abcam, ab51243), p53 (1:200 dilution, Santa Cruz Biotechnology, sc-126), cyclin E (1:200 dilution, Santa Cruz Biotechnology, sc-198), and β-actin (1:200 dilution, Santa Cruz Biotechnology, sc-7210) primary antibodies. Blots were then incubated with horseradish peroxidase-conjugated anti-rabbit or anti-mouse secondary antibodies (ECL plus western blotting reagent pack, 1:10,000 dilution, GE Healthcare, RPN2124). The immune complex was detected with the Amersham ECL Plus western blotting Detection System (GE Healthcare, RPN2132). The blots were exposed to Hyperfilm (Amersham Pharmacia Biotech), and bands were quantified with ImageJ densitometry software (National Institutes of Health).

DNA methylation pattern assay. Genomic DNA from HMEC at passage 12 was isolated using the Qiagen DNeasy kit according to the manufacturer's instructions. Differentially methylated fractions of DNA were then prepared using a Methyl-Profiler DNA Methylation Enzyme Kit (SA Biosciences). After DNA had been digested, digested DNA samples were prepared with real-time PCR using a Methyl-Profiler DNA Methylation PCR Array (SA Biosciences, MEAH-011A). The MEAH-011A was loaded with 24 gene promoters.

Bioinformatics and statistical analysis. Gene networks representing key genes for BPA exposure were identified using GNCPro (SA Biosciences), which is a free online software and an in silico research tool for collating gene and pathway interactions with integrating collective biological knowledge through text mining, data mining, data acquisition and computational prediction. The interactions among a group of genes are represented graphically and are interactive. All experiments in this study were performed independently two or more times to test the reproducibility of the results. Quantitative data are expressed as the means ± SD, except those for mRNA expression levels, which are expressed as the mean of two independent experiments. A non-parametric test, the Mann-Whitney U test, was applied to test for statistical significance. Values of $p < 0.05$ were considered to indicate statistical significance.

Disclosure of Potential Conflicts of Interest

No potential conflicts of interest were disclosed.

Acknowledgments

This study was supported in part by a Grant-in-Aid for Scientific Research from the Ministry of the Health and Labor, Japan. The authors gratefully acknowledge the critical advice of Dr. Tohru Inoue (National Institute of Health Sciences, Japan), and the technical support of Ms. Noriko Oshima (GE Healthcare Japan Corporation) in the analysis using the IN Cell Analyzer 1000. The authors also thank Ms. Yumi Matsumoto for her technical assistance.

Supplementary Material

Supplemental material can be found at:
www.landesbioscience.com/journals/cbt/article/18942/

References

1. Vandenberg LN, Hauser R, Marcus M, Olea N, Welshons WV. Human exposure to bisphenol A (BPA). Reprod Toxicol 2007; 24:139-77; PMID:17825522; http://dx.doi.org/10.1016/j.reprotox.2007.07.010.
2. Brotons JA, Olea-Serrano MF, Villalobos M, Pedraza V, Olea N. Xenoestrogens released from lacquer coatings in food cans. Environ Health Perspect 1995; 103:608-12; PMID:7556016; http://dx.doi.org/10.1289/ehp.95103608.
3. Calafat AM, Kuklenyik Z, Reidy JA, Caudill SP, Ekong J, Needham LL. Urinary concentrations of bisphenol A and 4-nonylphenol in a human reference population. Environ Health Perspect 2005; 113:391-5; PMID:15811827; http://dx.doi.org/10.1289/ehp.7534.
4. Krishnan AV, Stathis P, Permuth SF, Tokes L, Feldman D. Bisphenol-A: an estrogenic substance is released from polycarbonate flasks during autoclaving. Endocrinology 1993; 132:2279-86; PMID:8504731; http://dx.doi.org/10.1210/en.132.6.2279.
5. Keri RA, Ho SM, Hunt PA, Knudsen KE, Soto AM, Prins GS. An evaluation of evidence for the carcinogenic activity of bisphenol A. Reprod Toxicol 2007; 24:240-52; PMID:17706921; http://dx.doi.org/10.1016/j.reprotox.2007.06.008.
6. Markey CM, Luque EH, Munoz De Toro M, Sonnenschein C, Soto AM. In utero exposure to bisphenol A alters the development and tissue organization of the mouse mammary gland. Biol Reprod 2001; 65:1215-23; PMID:11566746.
7. Weber Lozada K, Keri RA. Bisphenol A increases mammary cancer risk in two distinct mouse models of breast cancer. Biol Reprod 2011; 85:490-7; PMID:21636739; http://dx.doi.org/10.1095/biolreprod.110.090431.
8. Lamartiniere CA, Jenkins S, Betancourt AM, Wang J, Russo J. Exposure to the endocrine disruptor bisphenol a alters susceptibility for mammary cancer. Horm Mol Biol Clin Investig 2011; 5:45-52; PMID:21687816; http://dx.doi.org/10.1515/HMBCI.2010.075.
9. Ptak A, Wrobel A, Gregoraszczuk EL. Effect of bisphenol-A on the expression of selected genes involved in cell cycle and apoptosis in the OVCAR-3 cell line. Toxicol Lett 2011; 202:30-5; PMID:21277958; http://dx.doi.org/10.1016/j.toxlet.2011.01.015.
10. Dairkee SH, Seok J, Champion S, Sayeed A, Mindrinos M, Xiao W, et al. Bisphenol A induces a profile of tumor aggressiveness in high-risk cells from breast cancer patients. Cancer Res 2008; 68:2076-80; PMID:18381411; http://dx.doi.org/10.1158/0008-5472.CAN-07-6526.
11. Singleton DW, Feng Y, Yang J, Puga A, Lee AV, Khan SA. Gene expression profiling reveals novel regulation by bisphenol-A in estrogen receptor-alpha-positive human cells. Environ Res 2006; 100:86-92; PMID:16029874; http://dx.doi.org/10.1016/j.envres.2005.05.004.
12. Diel P, Olff S, Schmidt S, Michna H. Effects of the environmental estrogens bisphenol A, o,p'-DDT, p-tert-octylphenol and coumestrol on apoptosis induction, cell proliferation and the expression of estrogen sensitive molecular parameters in the human breast cancer cell line MCF-7. J Steroid Biochem Mol Biol 2002; 80:61-70; PMID:11867264; http://dx.doi.org/10.1016/S0960-0760(01)00173-X.
13. Weng YI, Hsu PY, Liyanarachchi S, Liu J, Deatherage DE, Huang YW, et al. Epigenetic influences of low-dose bisphenol A in primary human breast epithelial cells. Toxicol Appl Pharmacol 2010; 248:111-21; PMID:20678512; http://dx.doi.org/10.1016/j.taap.2010.07.014.
14. Serrano M, Blasco MA. Cancer and ageing: convergent and divergent mechanisms. Nat Rev Mol Cell Biol 2007; 8:715-22; PMID:17717516; http://dx.doi.org/10.1038/nrm2242.
15. Collado M, Blasco MA, Serrano M. Cellular senescence in cancer and aging. Cell 2007; 130:223-33; PMID:17662938; http://dx.doi.org/10.1016/j.cell.2007.07.003.

16. Iso T, Futami K, Iwamoto T, Furuichi Y. Modulation of the expression of bloom helicase by estrogenic agents. Biol Pharm Bull 2007; 30:266-71; PMID:17268063; http://dx.doi.org/10.1248/bpb.30.266.
17. Bouskine A, Nebout M, Brucker-Davis F, Benahmed M, Fenichel P. Low doses of bisphenol A promote human seminoma cell proliferation by activating PKA and PKG via a membrane G-protein-coupled estrogen receptor. Environ Health Perspect 2009; 117:1053-8; PMID:19654912.
18. Moral R, Wang R, Russo IH, Lamartiniere CA, Pereira J, Russo J. Effect of prenatal exposure to the endocrine disruptor bisphenol A on mammary gland morphology and gene expression signature. J Endocrinol 2008; 196:101-12; PMID:18180321; http://dx.doi.org/10.1677/JOE-07-0056.
19. de Waard WJ, Aarts JM, Peijnenburg AA, Baykus H, Talsma E, Punt A, et al. Gene expression profiling in Caco-2 human colon cells exposed to TCDD, benzo[a]pyrene and natural Ah receptor agonists from cruciferous vegetables and citrus fruits. Toxicol In Vitro 2008; 22:396-410; PMID:18061397; http://dx.doi.org/10.1016/j.tiv.2007.10.007.
20. Buterin T, Koch C, Naegeli H. Convergent transcriptional profiles induced by endogenous estrogen and distinct xenoestrogens in breast cancer cells. Carcinogenesis 2006; 27:1567-78; PMID:16474171; http://dx.doi.org/10.1093/carcin/bgi339.
21. Garbe JC, Holst CR, Bassett E, Tlsty T, Stampfer MR. Inactivation of p53 function in cultured human mammary epithelial cells turns the telomere-length dependent senescence barrier from agonescence into crisis. Cell Cycle 2007; 6:1927-36; PMID:17671422; http://dx.doi.org/10.4161/cc.6.15.4519.
22. Stampfer MR, Bartley JC. Induction of transformation and continuous cell lines from normal human mammary epithelial cells after exposure to benzo[a]pyrene. Proc Natl Acad Sci USA 1985; 82:2394-8; PMID:3857588; http://dx.doi.org/10.1073/pnas.82.8.2394.
23. Sudo H, Garbe J, Stampfer MR, Barcellos-Hoff MH, Kronenberg A. Karyotypic instability and centrosome aberrations in the progeny of finite life-span human mammary epithelial cells exposed to sparsely or densely ionizing radiation. Radiat Res 2008; 170:23-32; PMID:18582160; http://dx.doi.org/10.1667/RR1317.1.
24. Qin XY, Zaha H, Nagano R, Yoshinaga J, Yonemoto J, Sone H. Xenoestrogens downregulate aryl-hydrocarbon receptor nuclear translocator 2 mRNA expression in human breast cancer cells via an estrogen receptor alpha-dependent mechanism. Toxicol Lett 2011; 206:152-7; PMID:21771643; http://dx.doi.org/10.1016/j.toxlet.2011.07.007.
25. Wetherill YB, Akingbemi BT, Kanno J, McLachlan JA, Nadal A, Sonnenschein C, et al. In vitro molecular mechanisms of bisphenol A action. Reprod Toxicol 2007; 24:178-98; PMID:17628395; http://dx.doi.org/10.1016/j.reprotox.2007.05.010.
26. Nijjar T, Bassett E, Garbe J, Takenaka Y, Stampfer MR, Gilley D, et al. Accumulation and altered localization of telomere-associated protein TRF2 in immortally transformed and tumor-derived human breast cells. Oncogene 2005; 24:3369-76; PMID:15735711; http://dx.doi.org/10.1038/sj.onc.1208482.
27. Kenny PA, Lee GY, Myers CA, Neve RM, Semeiks JR, Spellman PT, et al. The morphologies of breast cancer cell lines in three-dimensional assays correlate with their profiles of gene expression. Mol Oncol 2007; 1:84-96; PMID:18516279; http://dx.doi.org/10.1016/j.molonc.2007.02.004.
28. Jones PA, Baylin SB. The fundamental role of epigenetic events in cancer. Nat Rev Genet 2002; 3:415-28; PMID:12042769.
29. Fleming JM, Miller TC, Meyer MJ, Ginsburg E, Vonderhaar BK. Local regulation of human breast xenograft models. J Cell Physiol 2010; 224:795-806; PMID:20578247; http://dx.doi.org/10.1002/jcp.22190.
30. Bruder ED, Lee JJ, Widmaier EP, Raff H. Microarray and real-time PCR analysis of adrenal gland gene expression in the 7-day-old rat: effects of hypoxia from birth. Physiol Genomics 2007; 29:193-200; PMID:17213367; http://dx.doi.org/10.1152/physiolgenomics.00245.2006.
31. Evron E, Dooley WC, Umbricht CB, Rosenthal D, Sacchi N, Gabrielson E, et al. Detection of breast cancer cells in ductal lavage fluid by methylation-specific PCR. Lancet 2001; 357:1335-6; PMID:11343741; http://dx.doi.org/10.1016/S0140-6736(00)04501-3.
32. Fackler MJ, McVeigh M, Evron E, Garrett E, Mehrotra J, Polyak K, et al. DNA methylation of RASSF1A, HIN-1, RAR-beta, Cyclin D2 and Twist in in situ and invasive lobular breast carcinoma. Int J Cancer 2003; 107:970-5; PMID:14601057; http://dx.doi.org/10.1002/ijc.11508.
33. Lee JS, Fackler MJ, Teo WW, Lee JH, Choi C, Park MH, et al. Quantitative promoter hypermethylation profiles of ductal carcinoma in situ in North American and Korean women: Potential applications for diagnosis. Cancer Biol Ther 2008; 7:1398-406; PMID:18769130; http://dx.doi.org/10.4161/cbt.7.9.6425.
34. Romanov SR, Kozakiewicz BK, Holst CR, Stampfer MR, Haupt LM, Tlsty TD. Normal human mammary epithelial cells spontaneously escape senescence and acquire genomic changes. Nature 2001; 409:633-7; PMID:11214324; http://dx.doi.org/10.1038/35054579.
35. Sarkar P, Shiizaki K, Yonemoto J, Sone H. Activation of telomerase in BeWo cells by estrogen and 2,3,7,8-tetrachlorodibenzo-p-dioxin in co-operation with c-Myc. Int J Oncol 2006; 28:43-51; PMID:16327978.
36. Bandyopadhyay D, Curry JL, Lin Q, Richards HW, Chen D, Hornsby PJ, et al. Dynamic assembly of chromatin complexes during cellular senescence: implications for the growth arrest of human melanocytic nevi. Aging Cell 2007; 6:577-91; PMID:17578512; http://dx.doi.org/10.1111/j.1474-9726.2007.00308.x.
37. Narita M, Nunez S, Heard E, Narita M, Lin AW, Hearn SA, et al. Rb-mediated heterochromatin formation and silencing of E2F target genes during cellular senescence. Cell 2003; 113:703-16; PMID:12809602; http://dx.doi.org/10.1016/S0092-8674(03)00401-X.
38. Malyavantham KS, Bhattacharya S, Barbeitos M, Mukherjee L, Xu J, Fackelmayer FO, et al. Identifying functional neighborhoods within the cell nucleus: proximity analysis of early S-phase replicating chromatin domains to sites of transcription, RNA polymerase II, HP1gamma, matrin 3 and SAF-A. J Cell Biochem 2008; 105:391-403; PMID:18618731; http://dx.doi.org/10.1002/jcb.21834.
39. Hayakawa T, Haraguchi T, Masumoto H, Hiraoka Y. Cell cycle behavior of human HP1 subtypes: distinct molecular domains of HP1 are required for their centromeric localization during interphase and metaphase. J Cell Sci 2003; 116:3327-38; PMID:12840071; http://dx.doi.org/10.1242/jcs.00635.
40. Minc E, Allory Y, Worman HJ, Courvalin JC, Buendia B. Localization and phosphorylation of HP1 proteins during the cell cycle in mammalian cells. Chromosoma 1999; 108:220-34; PMID:10460410; http://dx.doi.org/10.1007/s004120050372.
41. Vermeulen K, Van Bockstaele DR, Berneman ZN. The cell cycle: a review of regulation, deregulation and therapeutic targets in cancer. Cell Prolif 2003; 36:131-49; PMID:12814430; http://dx.doi.org/10.1046/j.1365-2184.2003.00266.x.
42. Sherr CJ. Cancer cell cycles. Science 1996; 274:1672-7; PMID:8939849; http://dx.doi.org/10.1126/science.274.5293.1672.
43. Roussel-Gervais A, Bilodeau S, Vallette S, Berthelet F, Lacroix A, Figarella-Branger D, et al. Cooperation between cyclin E and p27(Kip1) in pituitary tumorigenesis. Mol Endocrinol 2010; 24:1835-45; PMID:20660298; http://dx.doi.org/10.1210/me.2010-0091.
44. Minella AC, Clurman BE. Mechanisms of tumor suppression by the SCF(Fbw7). Cell Cycle 2005; 4:1356-9; PMID:16131838; http://dx.doi.org/10.4161/cc.4.10.2058.
45. Kitagawa K, Kotake Y, Kitagawa M. Ubiquitin-mediated control of oncogene and tumor suppressor gene products. Cancer Sci 2009; 100:1374-81; PMID:19459846; http://dx.doi.org/10.1111/j.1349-7006.2009.01196.x.
46. Hao B, Oehlmann S, Sowa ME, Harper JW, Pavletich NP. Structure of a Fbw7-Skp1-cyclin E complex: multisite-phosphorylated substrate recognition by SCF ubiquitin ligases. Mol Cell 2007; 26:131-43; PMID:17434132; http://dx.doi.org/10.1016/j.molcel.2007.02.022.
47. Koepp DM, Schaefer LK, Ye X, Keyomarsi K, Chu C, Harper JW, et al. Phosphorylation-dependent ubiquitination of cyclin E by the SCF(Fbw7) ubiquitin ligase. Science 2001; 294:173-7; PMID:11533444; http://dx.doi.org/10.1126/science.1065203.
48. Minella AC, Loeb KR, Knecht A, Welcker M, Varnum-Finney BJ, Bernstein ID, et al. Cyclin E phosphorylation regulates cell proliferation in hematopoietic and epithelial lineages in vivo. Genes Dev 2008; 22:1677-89; PMID:18559482; http://dx.doi.org/10.1101/gad.1650208.
49. Jenkins S, Wang J, Eltoum I, Desmond R, Lamartiniere CA. Chronic oral exposure to bisphenol a results in a non-monotonic dose response in mammary carcinogenesis and metastasis in mmtv-erbb2 mice. Environ Health Perspect 2011; 119:1604-9; PMID:21988766; http://dx.doi.org/10.1289/ehp.1103850.
50. Li H, Collado M, Villasante A, Strati K, Ortega S, Canamero M, et al. The Ink4/Arf locus is a barrier for iPS cell reprogramming. Nature 2009; 460:1136-9; PMID:19668188; http://dx.doi.org/10.1038/nature08290.
51. Eckhardt F, Lewin J, Cortese R, Rakyan VK, Attwood J, Burger M, et al. DNA methylation profiling of human chromosomes 6, 20 and 22. Nat Genet 2006; 38:1378-85; PMID:17072317; http://dx.doi.org/10.1038/ng1909.
52. Radpour R, Kohler C, Haghighi MM, Fan AX, Holzgreve W, Zhong XY. Methylation profiles of 22 candidate genes in breast cancer using high-throughput MALDI-TOF mass array. Oncogene 2009; 28:2969-78; PMID:19503099; http://dx.doi.org/10.1038/onc.2009.149.
53. Dejeux E, Ronneberg JA, Solvang H, Bukholm I, Geisler S, Aas T, et al. DNA methylation profiling in doxorubicin treated primary locally advanced breast tumours identifies novel genes associated with survival and treatment response. Mol Cancer 2010; 9:68; PMID:20338046; http://dx.doi.org/10.1186/1476-4598-9-68.
54. Pal R, Srivastava N, Chopra R, Gochhait S, Gupta P, Prakash N, et al. Investigation of DNA damage response and apoptotic gene methylation pattern in sporadic breast tumors using high throughput quantitative DNA methylation analysis technology. Mol Cancer 2010; 9:303; PMID:21092294; http://dx.doi.org/10.1186/1476-4598-9-303.
55. Moelans CB, Verschuur-Maes AH, van Diest PJ. Frequent promoter hypermethylation of BRCA2, BRCA1, MSH6, PAX5, PAX6 and WT1 in ductal carcinoma in situ and invasive breast cancer. J Pathol 2011; 225:222-31; PMID:21710692; http://dx.doi.org/10.1002/path.2930.
56. Shim YH, Kang GH, Ro JY. Correlation of p16 hypermethylation with p16 protein loss in sporadic gastric carcinomas. Lab Invest 2000; 80:689-95; PMID:10830779; http://dx.doi.org/10.1038/labinvest.3780072.
57. Taghavi N, Biramijamal F, Sotoudeh M, Khademi H, Malekzadeh R, Moaven O, et al. $p16^{INK4a}$ hypermethylation and p53, p16 and MDM2 protein expression in esophageal squamous cell carcinoma. BMC Cancer 2010; 10:138; PMID:20388212; http://dx.doi.org/10.1186/1471-2407-10-138.

58. Zang JJ, Xie F, Xu JF, Qin YY, Shen RX, Yang JM, et al. P16 gene hypermethylation and hepatocellular carcinoma: a systematic review and meta-analysis. World J Gastroenterol 2011; 17:3043-8; PMID:21799651; http://dx.doi.org/10.3748/wjg.v17.i25.3043.

59. Salvesen HB, Das S, Akslen LA. Loss of nuclear p16 protein expression is not associated with promoter methylation but defines a subgroup of aggressive endometrial carcinomas with poor prognosis. Clin Cancer Res 2000; 6:153-9; PMID:10656444.

FEBS Letters 585 (2011) 3310–3315

FEBS Letters

journal homepage: www.FEBSLetters.org

siRNA-mediated knockdown of aryl hydrocarbon receptor nuclear translocator 2 affects hypoxia-inducible factor-1 regulatory signaling and metabolism in human breast cancer cells

Xian-Yang Qin [a,b,1], Feifei Wei [c,1], Jun Yoshinaga [b], Junzo Yonemoto [a], Masaru Tanokura [c], Hideko Sone [a,*]

[a] Health Risk Research Section, Research Center for Environmental Risk, National Institute for Environmental Studies, 16-2 Onogawa, Tsukuba, Ibaraki 305-8506, Japan
[b] Department of Environmental Studies, Graduate School of Frontier Science, The University of Tokyo, 5-1-5 Kashiwanoha, Kashiwa, Chiba 270-8563, Japan
[c] Department of Applied Biological Chemistry, Graduate School of Agricultural and Life Sciences, The University of Tokyo, 1-1-1 Yayoi, Bunkyo-ku, Tokyo 113-8657, Japan

ARTICLE INFO

Article history:
Received 18 August 2011
Revised 9 September 2011
Accepted 13 September 2011
Available online 19 September 2011

Edited by Judit Ovádi

Keywords:
Aryl-hydrocarbon receptor nuclear translocator 2
Breast cancer
Hypoxia-inducible factor-1
Metabolomics
Nuclear magnetic resonance

ABSTRACT

Recent human studies found that the mRNA expression level of aryl-hydrocarbon receptor nuclear translocator 2 (ARNT2) was positively associated with the prognosis of breast cancer. In this study, we used small interfering RNA techniques to knockdown ARNT2 expression in MCF7 human breast cancer cells, and found that an almost 40% downregulation of ARNT2 mRNA expression increased the expression of sensitive to apoptosis gene (3.36-fold), and decreased the expression of von Hippel-Lindau (0.27-fold) and matrix metalloproteinase-1 (0.35-fold). The metabolite analysis revealed the contents of glucose, glycine, betaine, phosphocholine, pyruvate and lactate involved in the hypoxia-inducible factor (HIF)-1-dependent glycolytic pathway were significantly lower in cells treated with siARNT2. Our results suggested that ARNT2 might play an important role in the modulation of HIF-1-regulated signaling and metabolism.

1. Introduction

Aryl-hydrocarbon receptor nuclear translocator 2 (ARNT2) is a member of the basic helix-loop-helix Per-ARNT-SIM family of transcription factors [1] and acts as a common obligate partner for several other members of the family, including aryl hydrocarbon receptor (AHR) and hypoxia-inducible factor (HIF)-1α [2,3]. Although many of the functions of ARNT2 remain unknown, it is believed that ARNT2 plays important roles in tumor angiogenesis by forming functional HIF complexes [4]. A recent study showed that ARNT2 mRNA expression levels are positively correlated with the prognosis of breast cancer, and that the presence of ARNT2 was significantly associated with smaller tumor sizes ($P = 0.006$), relapse-free survival ($P = 0.027$), and overall survival ($P = 0.002$) 5 years after breast cancer diagnosis [5]. These perspective findings indicate a possible role of ARNT2 in cancer development, treatment and outcome; however, much of this has yet to be elucidated.

Metabolites are regarded as the end products of cellular regulatory processes, and their levels can be considered as the ultimate response of biological systems to genetic or environmental changes [6]. The metabolism of a solid tumor is significantly different from that of the surrounding normal tissue, with cancer cells shifting glucose metabolism from oxidative to glycolytic pathways [7]. This process is known as the Warburg effect, at the heart of which is the HIF-dependent (and in particular, HIF-1-dependent) transcriptional regulation of virtually all of the genes in the glycolytic pathway, including glucose transporters, glycolytic enzymes, and various proteins involved in lactate production and pyruvate metabolism [8]. Nuclear magnetic resonance (NMR)-based metabolic profiling and metabolomics, combined with multivariate statistical analysis, have been widely applied in various areas of research, including drug toxicology, biomarker discovery, functional genomics, and molecular pathology [9–13]. Compared to other analytical techniques, such as gas chromatography–mass

Abbreviations: ARNT2, aryl-hydrocarbon receptor nuclear translocator 2; BaP, benzo[*a*]pyrenes; Glut-1, glucose transporter 1; HIF, hypoxia-inducible factor; KEGG, Kyoto Encyclopedia of Genes and Genomes; MMP1, matrix metalloproteinase-1; NMR, nuclear magnetic resonance; OPLS-DA, orthogonal projection to latent structure discriminant analysis; PCA, principal component analysis; SAG, sensitive to apoptosis gene; siRNA, small interfering RNA; VHL, von Hippel-Lindau

* Corresponding author. Fax: +81 29 850 2546.
E-mail addresses: y_qin@envhlth.k.u-tokyo.ac.jp (X.-Y. Qin), aa097025@mail.ecc.u-tokyo.ac.jp (F. Wei), junyosh@k.u-tokyo.ac.jp (J. Yoshinaga), yonemoto@nies.go.jp (J. Yonemoto), amtanok@mail.ecc.u-tokyo.ac.jp (M. Tanokura), hsone@nies.go.jp (H. Sone).

[1] These two authors contributed equally to this work.

0014-5793/$36.00
doi:10.1016/j.febslet.2011.09.017

spectrometry or liquid chromatography–mass spectrometry, NMR has the advantage of a fully quantitative analysis (with minimal sample preparation) to achieve a quick, direct and comprehensive observation [14].

In this study, NMR-based metabolomics was employed to investigate whether dysregulated ARNT2 mRNA expression could affect HIF-1-regulated metabolism in MCF7 human breast cancer cells. To assess the potential function of ARNT2 in breast cancer, we utilized small interfering RNA (siRNA) to knockdown ARNT2 mRNA expression levels in MCF7 cells, and then investigated its effect on the HIF-1 regulated signaling and metabolism.

2. Materials and methods

2.1. Cell culture

MCF7 cells were obtained from the Cell Engineering Division of RIKEN BioResource Center (Tsukuba, Ibaraki, Japan). Cells were maintained in RPMI 1640 medium (Wako, Osaka, Japan) containing 10% fetal bovine serum (FBS) (Mediatech, Herndon, VA) and grown at 37 °C in a 5% CO_2 humidified incubator. For growth under steroid-free conditions, the cells were seeded in phenol red-free DMEM (MP Biomedicals, Solon, OH) containing 10% charcoal/dextran-treated FBS (Hyclone, Logan, UT). All culture media contained 100 U/ml penicillin/streptomycin and 2 mmol/l L-glutamine (Mediatech).

2.2. RNA interference

siRNA targeting human ARNT2 (5′-CCGAUGGAAUCAUCACAUUUU-3′) and a scrambled sequence were designed and purchased from Genolution Pharmaceuticals Inc. (Seoul, South Korea). MCF7 cells were plated in 96-well plates (1×10^4 cells/well) for cell viability analysis, 24-well plates (5×10^4 cells/well) for RNA isolation, and 100 mm dishes (1×10^6 cells/dish) for metabolite analysis in phenol red-free media 1 day prior to transfection. Cells were then transfected with 10 nM or 100 nM siARNT2 and the scrambled siRNA as a negative control using G-Fectin, as per the manufacturer's instructions (Genolution Pharmaceuticals). The transfected cells were then incubated at 37 °C for 72 h and cultured in phenol red-free media without siARNT2 for another 48 h before analysis.

2.3. Quantitative real-time reverse transcription-polymerase chain reaction (RT-PCR)

Total RNA was isolated from cell cultures using an RNeasy Kit (Qiagen, Valencia, CA), and their amounts, purity and integrity were evaluated using a UV spectrophotometer and an Agilent Bioanalyzer 2100 (Agilent Technologies, Palo Alto, CA). cDNA was then synthesized using a High Capacity RNA-to-cDNA Kit (Applied Biosystems, Foster City, CA) and amplified in triplicate using TaqMan® Gene Expression Master Mix (Applied Biosystems) as previously described [15]. TaqMan Gene Expression Assays (Applied Biosystems) used in this study were Hs00208298_m1 for ARNT2, Hs00231048_m1 for ARNT, and Hs99999903_m1 for beta-actin. The gene expression was normalized to beta-actin expression and set to 1.0 for control cells treated with scramble siRNA.

2.4. Cell viability assay

Cells were washed twice with cold phosphate-buffered saline (PBS, Gibco, Grand Island, NY) and then fixed in 4% neutralized paraformaldehyde solution for 30 min. Nuclear counter-staining was detected with Hoechst 33258 (Wako Pure Chemical Industries, Osaka, Japan) and high-content cellular fluorescence images were acquired using an automatic fluorescence microscope (IN Cell Analyzer 1000; GE Healthcare, Buckinghamshire, UK).

2.5. Human HIF-regulated cDNA plate array

A human HIF-regulated cDNA plate array was used to determine the effect of downregulated ARNT2 mRNA expression on HIF-1 signaling (AP-0111, Signosis Inc., Sunnyvale, CA), according to the manufacturer's instructions. Briefly, total RNA (2 μg) was first reverse transcribed into cDNA in the presence of biotin-dUTP. Target genes were then specifically captured to individual wells on the plate through a pre-coated gene-specific oligonucleotide. The captured cDNAs were then detected with streptavidin-horseradish peroxidase (HRP) by the addition of a HRP chemiluminescent substrate. The concentration of cDNA was directly proportional to the chemiluminescent intensity of the test sample. The luciferase activity was measured using an AB-2100 luminometer (Atto, Tokyo, Japan). Luciferase induction was normalized to beta-actin and set to 1.0 for control cells treated with scramble siRNA.

2.6. NMR sample preparation

For metabolite analysis, MCF7 cells were harvested, as previously reported [16]. Briefly, cells (approximately 1×10^7 cells) were pelleted and washed twice with cold PBS to remove any residual medium. Excess PBS was removed via two rounds of centrifugation at maximum speed. Cell pellets were then stored at −80 °C for subsequent extraction. Aqueous soluble metabolites were then extracted using a chloroform/methanol/water extraction method, as previously described [13].

2.7. NMR analysis

The one-dimensional (1D) ^{1}H NMR spectra were measured at 500 MHz on a Varian Unity INOVA-500 spectrometer. The H_2O signal was suppressed by the pre-saturation method. The acquisition parameters were as follows: number of data points, 64 k; spectral width, 8000 Hz; acquisition time, 4.000 s; delay time, 2.0 s; and number of scans, 256. Detailed methods have been described previously [17].

2.8. Processing of spectra and data reduction

All NMR spectra were processed with the program MestReNova (Version 5.3.0, MestReC, Santiago de Compostela, Spain), reduced into 0.04 ppm spectral buckets, aligned using the Correlation Optimized Warping method, and then normalized.

2.9. Identification of metabolites

Metabolites were identified in the NMR spectra by comparing their ^{1}H chemical shifts and coupling patterns with corresponding values of metabolites from publicly accessible data banks [12], including the BioMagRes data bank (http://www.bmrb.wisc.edu), the Metabolomics Database of Linkoping (http://www.mdl.imv.liu.se), and the Human Metabolome Data Bank (http://www.hmdb.ca).

2.10. Statistical and multivariate analysis

All experiments in this study were performed in triplicate to test the reproducibility of the results. Quantitative data were expressed as the mean ± S.D. Statistical analysis was performed by two-tailed Student's *t*-test. Relationships were considered statistically significant with $P < 0.05$. Unsupervised principal component analysis (PCA) was used to obtain a general overview of the variance of the metabolites, and supervised orthogonal projection

to latent structure discriminant analysis (OPLS-DA) was performed to obtain information about differences in the metabolite composition of samples in SIMCA-P+ (Version 12.0, Umetrics, Umeå, Sweden). The map of the metabolic pathways was obtained from the Kyoto Encyclopedia of Genes and Genomes (KEGG; http://www.genome.jp/kegg/), a publicly available, web-based tool.

3. Results

3.1. Knockdown of ARNT2 mRNA expression in MCF7 cells

This study focused on the potential function of ARNT2 in human breast cancer cells. First, we sought to downregulate the mRNA expression of ARNT2 in MCF7 cells using siRNA techniques, the effects of which were confirmed by gene expression analysis and a cell viability assay. As shown in Fig. 1A, siARNT2 treatment caused a dose-dependent downregulation of ARNT2 mRNA expression. When treated with 10 and 100 nM siARNT2 for 72 h, we observed nearly 40% and 60% reductions, respectively, in ARNT2 mRNA expression in MCF7 cells. No significant effect was observed in ARNT mRNA expression with siARNT2 treatment (Fig. 1A). Furthermore, according to the cell viability assay, a significant inhibition in cell growth (approximately 80%) was observed in MCF7 cells treated with 100 nM, but not 10 nM, siARNT2 for 72 h (Fig. 1B). Hoechst staining indicated that a high dose of siARNT2 treatment at 100 nM induced apoptosis in MCF7 cells (data not shown).

To avoid cytotoxicity, 10 nM siARNT2 was used in subsequent experiments to investigate the effects of ARNT2 mRNA downregulation on HIF-1-regulated signaling and metabolism in MCF7 cells.

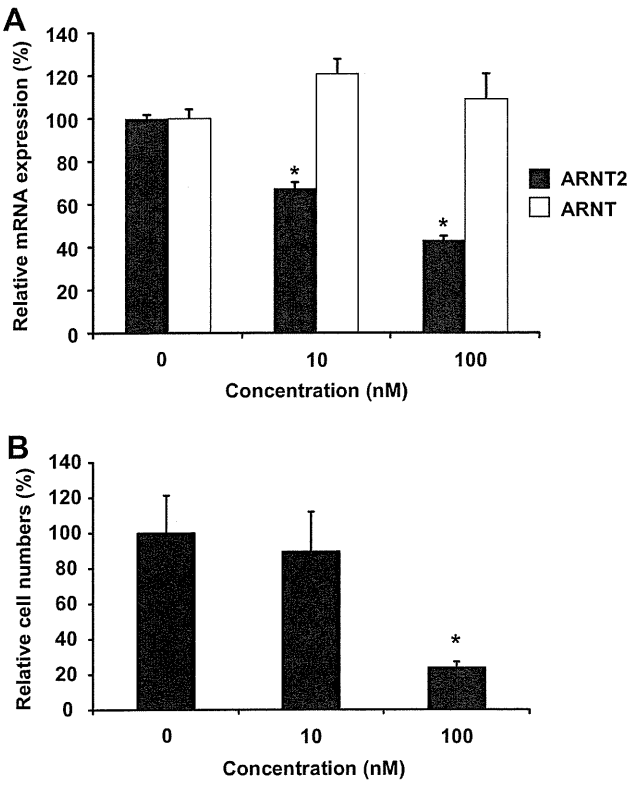

Fig. 1. siRNA-mediated downregulation of ARNT2 mRNA expression in MCF7 cells. Cells were treated with 10 and 100 nM siARNT2 for 72 h and then cultured for another 48 h in steroid-free media without siARNT2 treatment. Dose-dependent decreases in ARNT2 mRNA expression (A) and cell viability (B) following the siARNT2 treatment were confirmed. No significant effect was observed in ARNT mRNA expression with siARNT2 treatment (A). *$P < 0.05$ vs. the control cells treated with scramble siRNA.

3.2. Effects of ARNT2 mRNA downregulation in the expression of HIF signaling genes

A human HIF-regulated cDNA plate assay was used to measure the expression of HIF-1-regulated genes. The plate comprised a total of 21 genes involved in HIF-1 signaling. As shown in Fig. 2, downregulation of ARNT2 mRNA expression by 10 nM siARNT2 treatment for 72 h led to a 3.36-fold induction of sensitive to apoptosis gene (SAG) expression, and a 2-fold induction of Leptin expression. Furthermore, we observed a 0.27-fold and 0.35-fold reduction in von Hippel-Lindau (VHL) and matrix metalloproteinase-1 (MMP1) gene expression, respectively, as well as 0.5-fold reductions in glucose transporter 1 (Glut-1), Glut-3 and HIF-1α genes. These results indicated that ARNT2 may be involved in the modulation of HIF-1 signaling in MCF7 cells.

3.3. Metabolite profiling of MCF7 cells by ^{1}H NMR

A representative 1D ^{1}H NMR spectra of MCF7 cells without any treatment is shown (Fig. 3). Most of the information is located in the upfield region between 0.7 and 4.7 ppm (Fig. 3A), which corresponds to low molecular weight endogenous metabolites. The major metabolite classes observed included amino acids (e.g., alanine, valine, and tyrosine), organic osmolytes (e.g., betaine and glycine), organic acids (e.g., acetic acid), carbohydrates (e.g., glucose), nucleotides (e.g., ATP), and glycolytic products (e.g., lactate and pyruvate).

3.4. Effects of downregulation of ARNT2 mRNA expression in the metabolism of MCF7 cells

To determine which metabolites significantly correlated with the downregulation of ARNT2 mRNA expression, PCA and OPLS-DA modelings were applied to the ^{1}H NMR spectra of six independent data sets from control cells and cells with siARNT2 treatment ($n = 3$, respectively). PCA is a standard technique of pattern recognition and multivariate data analysis. The scores plot (PC 1 vs. 2) discriminated between the intracellular metabolites of control cells and cells treated with siARNT2 (Fig. 4A). It should be noted that these differences were identified using an unsupervised analysis, without any prior information about the samples. Since all

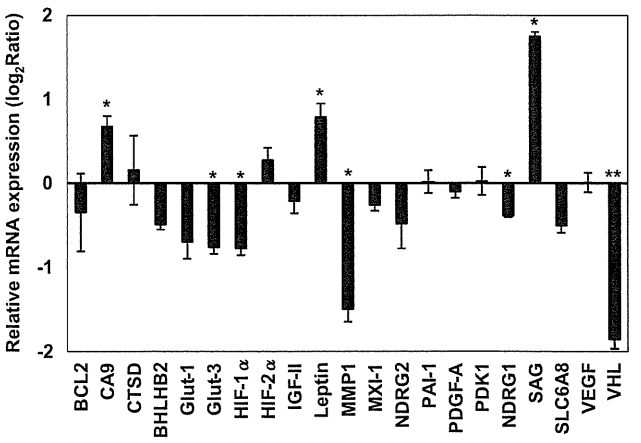

Fig. 2. Effects of downregulation of ARNT2 mRNA expression in the expression of HIF signaling genes in MCF7 cells. Cells were treated with 10 nM siARNT2 for 72 h and then cultured for another 48 h in steroid-free media without siARNT2 treatment. The expression of HIF signaling genes was then measured using a human HIF-regulated cDNA plate assay (Signosis). Relative mRNA expression normalized to beta-actin was shown as $\log_2$ ratio, with the fold-change referring to the control cells. *$P < 0.05$, **$P < 0.01$ vs. the control cells treated with scramble siRNA.

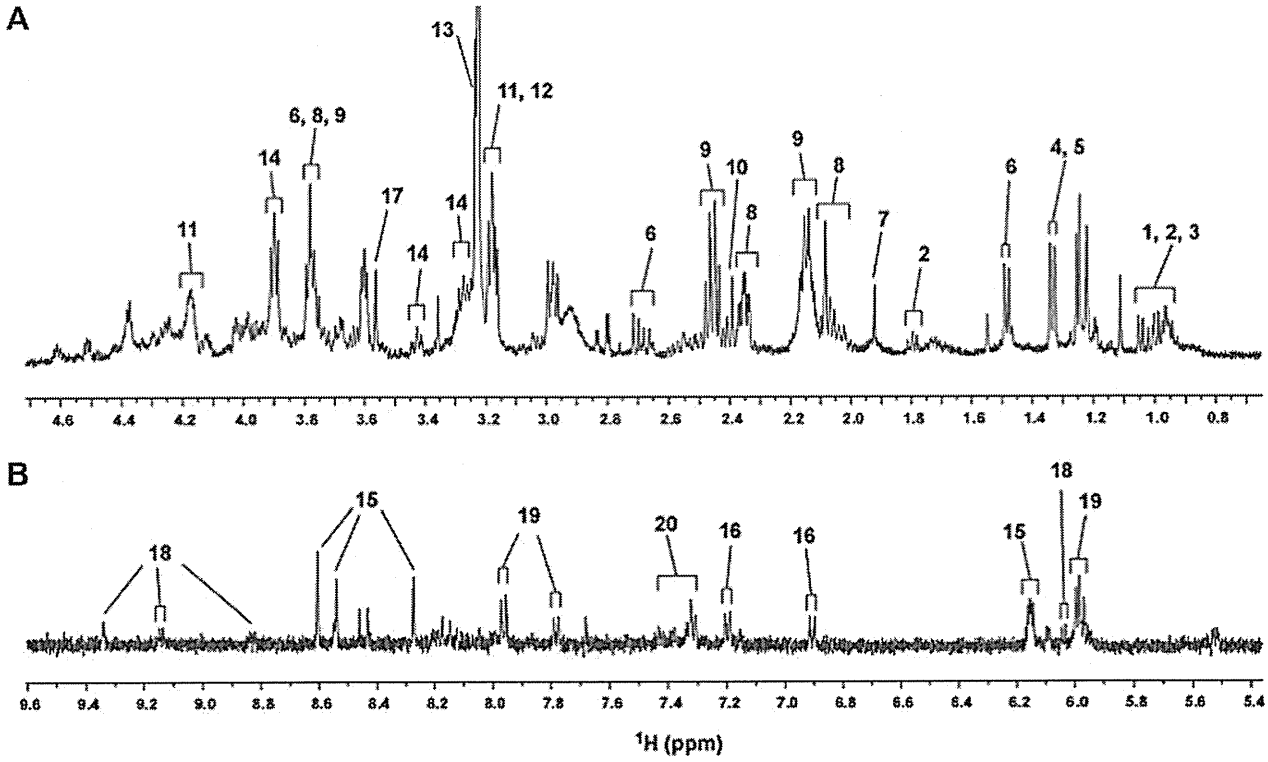

Fig. 3. Assignment of 1D NMR spectra of MCF7 cells. (A) Expansion of the ^{1}H NMR spectrum from 0.7 to 4.7 ppm. (B) Expansion of the ^{1}H NMR spectrum from 5.4 to 9.6 ppm. Metabolites: 1, isoleucine; 2, leucine; 3, valine; 4, lactic acid (lactate); 5, threonine; 6, alanine; 7, acetic acid (acetate); 8, glutamate; 9, glutamine; 10, pyruvic acid (pyruvate); 11, phosphocholine; 12, glycerophosphocholine; 13, betaine; 14, glucose; 15, ATP/ADP/AMP; 16, tyrosine; 17, glycine; 18, NAD+/NADP+; 19, 4-nitrophenol; 20, phenylalanine.

cells were cultured under identical conditions, the observed discrimination demonstrates that the downregulation of ARNT2 mRNA expression is strongly represented by the individual metabolic profiles.

In contrast to PCA, OPLS-DA is a supervised method that explains maximum separation between pre-defined classes in the data. In this case, the scores plot separated control cells and cells treated with siARNT2 along the discriminating t[1] (data not shown). Potential biomarkers for the separation were subsequently identified using S-plot, which were represented with covariance (p) against correlation ($p$corr). The S-plot of the OPLS-DA showed the most relevant variables in the differentiation of two samples, and the identified biomarkers are highlighted in Fig. 4B. The levels of betaine, glucose, glycine, phosphocholine, pyruvate, lactate and ATP/ADP/AMP were significantly decreased in cells with siARNT2 treatment, indicating that the downregulation of ARNT2 mRNA expression may impair HIF-1-regulated glycine synthesis and glucose metabolism in MCF7 cells.

4. Discussion

ARNT2 function is hypothesized to be related to organ development, since Arnt2 knockout mice and zebrafish suffer severe developmental defects and die shortly after birth [18,19]. Compared to its homolog ARNT, ARNT2 is reported to have a more restricted pattern of expression, commonly found in the central nervous system and other developing organs, such as the kidney [4]. However, recent studies have found a increased frequency of ARNT2 transcripts in tumor specimens from primary breast cancer patients, as compared with normal breast tissue samples. Moreover, the mRNA expression levels of ARNT2 correlate significantly with favorable disease outcomes for breast cancer patients, suggesting ARNT2 might be associated with cancer development, treatment and outcome [5]. In this study, we sought to investigate the potential function of ARNT2 in HIF-1-regulated signaling and metabolism in breast cancer, using siRNA to knockdown ARNT2 mRNA expression in MCF7 cells.

HIF-1 regulates numerous pathways that are potentially important for tumor growth, including angiogenesis and glycolysis [20]. Whilst much attention has focused on its role in the cellular response to hypoxia, HIF-1 is also constitutively expressed in many tumors [21]. HIF-1 is a heterodimeric transcription factor composed of HIF-1α, which dimerizes with a constitutively expressed β-subunit, such as ARNT and ARNT2, and subsequently binds to hypoxia response elements in the promoters of target genes [4,8]. HIF-1α expression in cells is known to be regulated by a variety of stimuli, including fluctuations in cellular oxygen concentration, growth factors, oncogenic activation, or loss of tumor suppressor function [22]. In this study, knockdown of ARNT2 mRNA expression significantly decreased HIF-1α expression (0.58-fold, $P = 0.049$), while no significant effect was found with HIF-2α expression (1.25-fold, $P = 0.60$). Although HIF-1α and HIF-2α share similar protein structure and are both key transcriptional regulators of the hypoxic response, several physiological and mechanistic differences between HIF-1α and HIF-2α have been reported [23]. A recent study found a switch in HIF-1α- to HIF-2α-dependent signaling in cancer cells, and that overexpression of the E3-ubiquitin ligase, hypoxia-associated factor, could decrease HIF-1α levels but not HIF-2α in normoxic or hypoxic conditions [24]. Our findings suggest that ARNT2 might be a potential mediator of HIF-1, but not HIF-2, signaling pathways in MCF7 cells; however, the precise mechanism of action remains to be determined.

We observed significant changes to the expressions of several other proteins in response to ARNT2 knockdown, including an increase in SAG expression, and decreases in VHL and MMP1

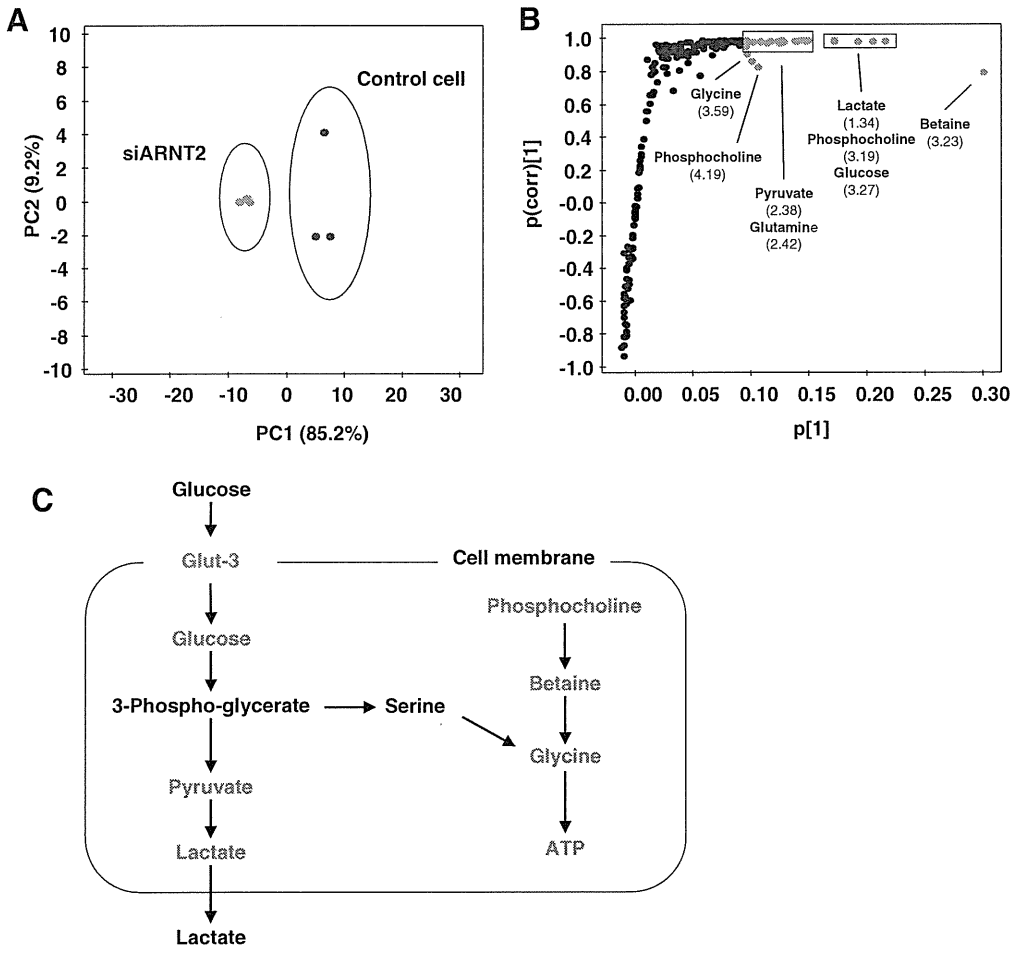

Fig. 4. Statical analysis of metabolites in MCF7 cells. Cells were treated with 10 nM siARNT2 for 72 h and then cultured for another 48 h in steroid-free media without siARNT2 treatment. PCA score plots (A) and OPLS-DA loading S-plots (B) were applied to the intercellular metabolic profiles to assess siARNT2 treatment-related effects. Blue and orange are used to mark control cells and cells treated with siARNT2 in the PCA score plots, respectively. Key metabolites (orange) related with glycine synthesis and glucose metabolism were highlighted in the S-plot. Schematic representation of the metabolic pathways showing the most relevant metabolic changes induced by siARNT2 treatment was summarized according to KEGG metabolism map (C). Blue and green are used to mark downregulated genes and metabolites following siARNT2 treatment, respectively. Metabolites that do not show any significant changes or for which there are no measurements in this study are shown in black.

expressions. VHL is a well-known tumor suppressor, and inactivation of VHL has been implicated in the pathogenesis of several cancers [25]. The cellular levels of HIF-1α are tightly regulated via post-translation modification by prolyl hydroxylases and the VHL, Cullin and Elongin B/C E3-ubiquitin ligase [26]. Furthermore, in renal carcinoma cells, VHL has been shown to negatively regulate HIF-1α and other hypoxia-inducible genes [25,27]. When VHL expression is lost in renal cancers, HIF-1α is constitutively stable (even in normoxia), resulting in constitutive transcription of its target genes and the loss of VHL-mediated tumor suppression. In our study, the knockdown of ARNT2 mRNA expression inhibited VHL expression, which, in turn, activated HIF-1α signaling.

We observed an increase in SAG expression in response to ARNT2 knockdown in MCF7 cells. SAG encodes a redox-inducible and apoptosis-protective antioxidant protein that, when overexpressed, protects mammalian cells from hypoxia-induced apoptosis [26]. A HIF-1-SAG feedback loop has been reported previously, where the inactivation of VHL induces HIF-1 to transactivate SAG, which, in turn, mediates the ubiquitination and degradation of HIF-1α [26]. This feedback loop is in accordance with our observations. In addition, the inhibition of HIF-1α may have caused the decrease in MMP1 that we observed, and potentially other hypoxia-inducible genes [28,29]. It should be noted that the knockdown of ARNT2 expression showed differential effects on the transcriptions of HIF-target genes (as shown in Fig. 2). Although several factors involved in the regulation of gene expression might contribute to this, including differences in the promoter structure and binding affinity, further study is warranted to ascertain the underlying mechanism of action.

Numerous reports have alluded to the shift in glucose metabolism that occurs in cancer cells: from oxidative to glycolytic pathways, in the presence of oxygen [7]. This process is known as the Warburg effect, where HIF-1α-dependent transcriptional regulation of virtually all of the genes in the glycolytic pathways lies at the center of this effect, including the regulation of glucose transporters, glycolytic enzymes, proteins involved in lactate production and others involved in pyruvate metabolism [8]. Our gene expression analysis found that the downregulation of ARNT2 mRNA expression in MCF7 cells significantly inhibited the expression of Glut-3: a predominant glucose transporter responsible for glucose uptake in neurons and cancer cells. This finding indicates that ARNT2 may regulate HIF-1-mediated glucose and energy metabolism [29]. Our metabolite analysis lends further support to this hypothesis, with significant decreases in glycine, an essential precursor of ATP synthesis, as well as other intermediates related to glycine synthesis (phosphocholine and betaine) in cells treated with siARNT2. Moreover, the breakdown products of pyruvate and lactate were also decreased following siARNT2 treatment. Our results suggest that the knockdown of ARNT2 mRNA expression may disrupt HIF-1-regulated glucose and energy metabolism

by inhibiting the expression of hypoxia-inducible genes, such as Glut-3 (Fig. 4C). These observations are in agreement with previous studies, suggesting that disruption of the HIF-1 pathway in tumor cells could impair the supply of anabolic precursors required for cell synthesis [7,21].

In our previous study, we showed that xenoestrogens, such as bisphenol A (BPA), can downregulate ARNT2 mRNA and protein expressions in MCF7 cells [15]. Combined with these new findings, it is plausible to suggest that prenatal and/or long-term chronic exposure to xenoestrogens could affect human fetal health by impairing ARNT2 function, without any significant symptoms, until the accumulated effects possibly lead to tumorigenesis in later life. This may be of particular importance because humans are still widely exposed to xenoestrogens. For example, BPA is still produced worldwide and employed in the manufacture of commonly used polycarbonate plastic products and personal care products [30].

ARNT2 is involved in numerous other physiological pathways, such as in AHR signaling, which is important in the metabolic activation and detoxification of ubiquitous environmental pollutants and carcinogens, including dioxins and benzo[*a*]pyrenes (BaP) [1–3]. Interestingly, a recent study reported a two-way interaction between HIF-1 and AHR pathways, where HIF-1α activation significantly reduced the levels of AHR downstream targets genes and increased BaP-induced genetic instability [31]. Our results suggest that ARNT2 may play a role in cancer development by a HIF-1-mediated mechanism that perhaps also includes the modulation of AHR signaling and carcinogen metabolism. However, the details of this mechanism of action are still unclear, and further experimentation is warranted.

5. Conclusions

In summary, we described a role for ARNT2 in the modulation of HIF-1-regulated signaling and metabolism in MCF7 cells. ARNT2 is an essential regulator involved in the physiological response to several critical environmental insults, including chemical toxins and hypoxia. The regulatory effects of ARNT2 on the tumor suppressor activity of VHL and the anti-apoptosis activity of SAG suggest the potential role of ARNT2 in cancer development, treatment and outcome. However, a detailed mechanism of action is still unclear from this limited study, and further research to elucidate the functions of ARNT2 in more detail is necessary in epidemiology studies and in different in vivo and in vitro models.

Acknowledgment

This study was supported in part by the Environmental Technology Development Fund from the Ministry of the Environment, Japan.

References

[1] Hirose, K., Morita, M., Ema, M., Mimura, J., Hamada, H., Fujii, H., Saijo, Y., Gotoh, O., Sogawa, K. and Fujii-Kuriyama, Y. (1996) CDNA cloning and tissue-specific expression of a novel basic helix-loop-helix/PAS factor (Arnt2) with close sequence similarity to the aryl hydrocarbon receptor nuclear translocator (Arnt). Mol. Cell. Biol. 16, 1706–1713.
[2] Sekine, H., Mimura, J., Yamamoto, M. and Fujii-Kuriyama, Y. (2006) Unique and overlapping transcriptional roles of arylhydrocarbon receptor nuclear translocator (Arnt) and Arnt2 in xenobiotic and hypoxic responses. J. Biol. Chem. 281, 37507–37516.
[3] Hankinson, O. (2008) Why does ARNT2 behave differently from ARNT? Toxicol. Sci. 103, 1–3.
[4] Maltepe, E., Keith, B., Arsham, A.M., Brorson, J.R. and Simon, M.C. (2000) The role of ARNT2 in tumor angiogenesis and the neural response to hypoxia. Biochem. Biophys. Res. Commun. 273, 231–238.
[5] Martinez, V., Kennedy, S., Doolan, P., Gammell, P., Joyce, H., Kenny, E., Prakash Mehta, J., Ryan, E., O'Connor, R., Crown, J., Clynes, M. and O'Driscoll, L. (2008) Drug metabolism-related genes as potential biomarkers: analysis of expression in normal and tumour breast tissue. Breast Cancer Res. Treat. 110, 521–530.
[6] Fiehn, O. (2002) Metabolomics—the link between genotypes and phenotypes. Plant Mol. Biol. 48, 155–171.
[7] Denko, N.C. (2008) Hypoxia, HIF1 and glucose metabolism in the solid tumour. Nat. Rev. Cancer 8, 705–713.
[8] Rankin, E.B. and Giaccia, A.J. (2008) The role of hypoxia-inducible factors in tumorigenesis. Cell Death Differ. 15, 678–685.
[9] Reo, N.V. (2002) NMR-based metabolomics. Drug Chem. Toxicol. 25, 375–382.
[10] Coen, M., Holmes, E., Lindon, J.C. and Nicholson, J.K. (2008) NMR-based metabolic profiling and metabonomic approaches to problems in molecular toxicology. Chem. Res. Toxicol. 21, 9–27.
[11] Weljie, A.M., Bondareva, A., Zang, P. and Jirik, F.R. (2011) ^{1}H NMR metabolomics identification of markers of hypoxia-induced metabolic shifts in a breast cancer model system. J. Biomol. NMR 49, 185–193.
[12] Cano, K.E., Li, Y.J. and Chen, Y. (2010) NMR metabolomic profiling reveals new roles of SUMOylation in DNA damage response. J. Proteome Res. 9, 5382–5388.
[13] Ellis, J.K., Athersuch, T.J., Cavill, R., Radford, R., Slattery, C., Jennings, P., McMorrow, T., Ryan, M.P., Ebbels, T.M. and Keun, H.C. (2011) Metabolic response to low-level toxicant exposure in a novel renal tubule epithelial cell system. Mol. BioSyst. 7, 247–257.
[14] Griffin, J.L. (2003) Metabonomics: NMR spectroscopy and pattern recognition analysis of body fluids and tissues for characterisation of xenobiotic toxicity and disease diagnosis. Curr. Opin. Chem. Biol. 7, 648–654.
[15] Qin, X.Y., Zaha, H., Nagano, R., Yoshinaga, J., Yonemoto, J. and Sone, H. (2011) Xenoestrogens down-regulate aryl-hydrocarbon receptor nuclear translocator 2 mRNA expression in human breast cancer cells via an estrogen receptor alpha-dependent mechanism. Toxicol. Lett. 206, 152–157.
[16] Sheikh, K.D., Khanna, S., Byers, S.W., Fornace Jr., A. and Cheema, A.K. (2011) Small molecule metabolite extraction strategy for improving LC/MS detection of cancer cell metabolome. J. Biomol. Tech. 22, 1–4.
[17] Wei, F., Furihata, K., Hu, F., Miyakawa, T. and Tanokura, M. (2010) Complex mixture analysis of organic compounds in green coffee bean extract by two-dimensional NMR spectroscopy. Mag. Res. Chem. 48, 857–865.
[18] Hosoya, T., Oda, Y., Takahashi, S., Morita, M., Kawauchi, S., Ema, M., Yamamoto, M. and Fujii-Kuriyama, Y. (2001) Defective development of secretory neurones in the hypothalamus of Arnt2-knockout mice. Genes Cells 6, 361–374.
[19] Hsu, H.J., Wang, W.D. and Hu, C.H. (2001) Ectopic expression of negative ARNT2 factor disrupts fish development. Biochem. Biophys. Res. Commun. 282, 487–492.
[20] Harris, A.L. (2002) Hypoxia—a key regulatory factor in tumour growth. Nat. Rev. Cancer 2, 38–47.
[21] Griffiths, J.R., McSheehy, P.M., Robinson, S.P., Troy, H., Chung, Y.L., Leek, R.D., Williams, K.J., Stratford, I.J., Harris, A.L. and Stubbs, M. (2002) Metabolic changes detected by in vivo magnetic resonance studies of HEPA-1 wild-type tumors and tumors deficient in hypoxia-inducible factor-1beta (HIF-1beta): evidence of an anabolic role for the HIF-1 pathway. Cancer Res. 62, 688–695.
[22] Carroll, V.A. and Ashcroft, M. (2006) Role of hypoxia-inducible factor (HIF)-1alpha versus HIF-2alpha in the regulation of HIF target genes in response to hypoxia, insulin-like growth factor-I, or loss of von Hippel-Lindau function: implications for targeting the HIF pathway. Cancer Res. 66, 6264–6270.
[23] Bracken, C.P., Fedele, A.O., Linke, S., Balrak, W., Lisy, K., Whitelaw, M.L. and Peet, D.J. (2006) Cell-specific regulation of hypoxia-inducible factor (HIF)-1α and HIF-2α stabilization and transactivation in a graded oxygen environment. J. Biol. Chem. 281, 22575–22585.
[24] Koh Jr., M.Y., Lemos, R., Liu, X. and Powis, G. (2011) The hypoxia-associated factor switches cells from HIF-1α- to HIF-2α-dependent signaling promoting stem cell characteristics, aggressive tumor growth and invasion. Cancer Res. 71, 4015–4027.
[25] Iliopoulos, O., Levy, A.P., Jiang, C., Kaelin Jr., W.G. and Goldberg, M.A. (1996) Negative regulation of hypoxia-inducible genes by the von Hippel-Lindau protein. Proc. Natl. Acad. Sci. USA 93, 10595–10599.
[26] Tan, M., Gu, Q., He, H., Pamarthy, D., Semenza, G.L. and Sun, Y. (2008) SAG/ROC2/RBX2 is a HIF-1 target gene that promotes HIF-1 alpha ubiquitination and degradation. Oncogene 27, 1404–1411.
[27] Baldewijns, M.M., van Vlodrop, I.J., Vermeulen, P.B., Soetekouw, P.M., van Engeland, M. and de Bruine, A.P. (2010) VHL and HIF signalling in renal cell carcinogenesis. J. Pathol. 221, 125–138.
[28] Sun, X., Wei, L., Chen, Q. and Terek, R.M. (2010) CXCR4/SDF1 mediate hypoxia induced chondrosarcoma cell invasion through ERK signaling and increased MMP1 expression. Mol. Cancer 9, 17.
[29] Liu, Y., Liu, F., Iqbal, K., Grundke-Iqbal, I. and Gong, C.X. (2008) Decreased glucose transporters correlate to abnormal hyperphosphorylation of tau in Alzheimer disease. FEBS Lett. 582, 359–364.
[30] Vandenberg, L.N., Hauser, R., Marcus, M., Olea, N. and Welshons, W.V. (2007) Human exposure to bisphenol A (BPA). Reprod. Toxicol. 24, 139–177.
[31] Schults, M.A., Timmermans, L., Godschalk, R.W., Theys, J., Wouters, B.G., van Schooten, F.J. and Chiu, R.K. (2010) Diminished carcinogen detoxification is a novel mechanism for hypoxia-inducible factor 1-mediated genetic instability. J. Biol. Chem. 285, 14558–14564.